Research Journal of Recent Sciences ISSN 2277-2502
Vol. **4(9),** 68-92, September **(2015)** *Res.J.Recent Sci.*

Earthquake time Signature in SST and SLHF through analysis of 20 major EQ events of West Pacific Zone

Athparia R.*, Devi M. and Barbara A.K.
Department of Physics, Gauhati University, Guwahati, INDIA

Available online at: www.isca.in, www.isca.me
Received 27th March 2015, revised 1st June 2015, accepted 6th July 2015

Abstract

The paper aims at identification of possible signatures of an impending earthquake (EQ) in parameters like surface latent heat flux (SLHF) and sea surface temperature (SST) by analysing 20 EQs with magnitude >6 occurring in the west pacific coastal and off coastal regions. For this purpose, SLHF magnitudes are taken from NCEP/ NCAR reanalysis data ($1.8^0 \times 1.8^0$ grid) and SST values are obtained from NOAA/ NCDC with grid size $0.25^0 \times 0.25^0$. The daily spatial SST and SLHF distribution obtained from NOAA is also examined over the epicenter zones of earthquake under consideration. The paper gives the detailed statistical approaches adopted for extracting EQ signatures in the two parameters considered here. The analysis starts with defining a parameter called Anomaly Index (AI) which is calculated by comparing the daily values of SST and SLHF over the epicenter area with the long term (10 yrs) average values of the parameters. While calculating the long term average values (x′), the data are exclusively screened for non-EQ days for periods two month prior to and one month after the occurrence of the event. The x′ values are compared with corresponding EQ day data (x) and the resultant magnitudes of X=(x-x′) are then normalised for removing non- EQ time influences by defining the anomaly parameter as $AI = \frac{(x-x')}{\sigma}$, where (σ) is the standard deviation of x' taking mean data value of each year. To identify EQ time anomaly, the mean (μ) and the standard deviation (s) is calculated from the fluctuations of AI values and only when the value crosses, μ+2σ limit, the situation is marked as EQ time anomaly over the earthquake region. The paper finally presents that prediction reliability of an impending earthquake through SST and SLHF anomaly to have regional and temporal influences.

Keywords: Earthquake, sea surface temperature, surface latent heat flux.

Introduction

It is well known that seismic activities associated with an earthquake (EQ) develop strains in the mantle of earth leading to modification in surface temperature, the result of which may be reflected in sea surface temperature (SST) and surface latent heat flux (SLHF) especially when epicentres lie in the ocean and coastal region. Therefore one can expect changes in these two parameter prior to and during an EQ event. In fact a significant amount of work has been done associating modifications observed in SLHF, SST prior to an impending EQ[1-7]. In this connection, references may be made of the works of Singh et al.[8,9], who have observed enhancement of near-surface temperature variations after the strong Gujarat EQ of January 26, 2001 and of Cervone et al.[10], who have reported SLHF anomaly 2 weeks before the EQs of August 14, 2003 and March 1, 2004 in Greece. Working over seven major earthquakes in the Indian region of M>5.5 Goswami et al.[11] have noted that SLHF shows an increase during earthquakes and that the effect is more pronounced in case of earthquakes with epicenter near to an ocean. Finally Goswami et al[11] reported that anomaly in SLHF depends on the season and the available moisture content in the earth's surface. It is however noted that with all these observations and analysis there are still scopes to look for a well defined EQ precursor from SST and SLHF variation and to understand role of EQ preparatory processes in modifying SST and SLHF. The purpose of this work is therefore to look for a well defined precursor of an impending EQ in SST and SLHF variations by examining 20 EQs of M>6.

Methodology

The SST and SLHF data for this study have been obtained from the National Centre for Environmental Prediction (NCEP). These SST data are available in resolution of global grid $0.25^0 \times 0.25^0$ and SLHF data are available in grid $1.8^0 \times 1.8^0$. The EQ events of greater than 6M are taken under study, their magnitude, depth and location of epicenter are taken from USGS are presented in table-1.

The following procedure is adapted for extraction of EQ time anomaly from SST and SLHF data.

The SST and SLHF magnitude (x) over the epicentre area is plotted for each day covering two months (m-2) prior to and one month (m+1) after the EQ. The long term (10 years) average values (x') for (m-2) and (m+1) months are then calculated. An anomaly parameter is then defined by the following equation:

$$AI = \frac{x-x'}{\sigma} \quad (1)$$

Where, σ is the standard deviation calculated from 10 years data. AI for m-2 and m+1 month are then plotted with mean value μ and standard deviation s and (μ+2s) is considered to be the background noise level and any fluctuation beyond this limit will be considered as an anomaly over the earthquake region under consideration.

Results and Discussion

Table 1 shows the detail of the EQs under consideration. In figures-1 to 6 a few cases of SST anomaly prior to EQ events under consideration are presented. In each figure the dotted red lines shows (μ+2s) value which is considered the maximum background noise and the black bar shows the EQ day. The increment in SST anomaly to the maximum has been observed to be 2-3 weeks prior to the main earthquake event. The equation numbers 1-9, 11, 14, 18 and 20 showed positive relation with EQ whereas numbers 10, 12, 13, 19 did not show any relation with EQ. Before the main earthquake event, SST value is found to be greater than the sum of the mean SST plus 2 times the standard deviations, which indicates that only before an earthquake does the SST value becomes significantly high. All the values found to lie within this range are therefore considered as background noise, but prior to the earthquake event, the value is found to be higher than maximum range of background noise. After the main earthquake event, the value has been found to decrease and then increase, before it acquires the average background value. Figure-7 shows the variation of maximum value of AI index (AI_{max}) for SST with the EQ magnitude and a significant positive co-relation with co-efficient of 0.65 is seen between the two parameter. The AI in case of SST is highly dependent on the magnitude of the earthquake and the location of epicenter. Figure-8 (a-m) shows the spatial distribution of SST anomaly in Nicobar region prior to and after the earthquake over the epicenter area. The magnitude of the anomaly on SST, observed over the epicenter area of an earthquake is highly variable and is controlled by the sea currents and prevailing atmospheric conditions over that region. Further the magnitude, depth, time and season of occurrence may also play significant role in modifying the SST variations. The physical processes behind the SST anomaly prior to the earthquake may be attributed to the crustal deformation due to the stress field. Due to the acting stress field, sub-surface pressure increases with the consequent increase in temperature[12]. The gases trapped in these pores escape, create a localized heating, and thus upwelling from the sea bottom to finally elevate the SST. A red color contour is observed on the south of the epicentre on 1st and 2nd June 2010. The migration of SST contrast seems to begin from this zone towards the epicentral region. The migration of strong SST contrast zone over the epicentral region is likely to be due to heat conduction through water. The SST anomaly is seen 2-3 weeks prior to earthquake. The strong SST contrast is seen over epicentral region on 4th and 5th June 2010 i.e. 7-8 days prior to the main event of 12th June 2010 with mean SST of magnitude 31.2^{0}C. Soon after the earthquake this strong SST contrast is found to disappear on 13th June with value 30^0 C.

Table-1
Earthquakes under consideration

EQ no.	Date	Time(UTC)	Lat.	long	Depth	Mag.	Location
1	12.8.2009	22:48:51	32.816°N	140.382°E	51	6.6	Japan
2	28.11.2004	18:32:13	42.995°N	145.056°E	39	7	Japan
3	10.11.2009	02:48:47	08.1°N	92.0°E	36	6.1	Andaman
4	12.9.2007	11:10:26	4.520°S	101.374°E	34	8.5	Southern Sumatra, Indonesia
5	17.7.2006	08:19:28	9.222°S	107.320°E	34	7.7	South of Java, Indonesia
6	6.4.2010	22:15:02	2.360°N	97.132°E	31	7.8	Northern Sumatara, Indonesia
7	26.12.2004	00:58:53	3.316°N	95.854°E	30	9.1	Northern Sumatara, Indonesia
8	11.3.2011	05:46:24	38.297°N	142.372°E	30	9	Japan
9	25.9.2003	19:50:06	41.775°N	143.904°E	27	8.3	Japan
10	11.4.2012	08:38:37	2.311°N	93.063°E	22.9	8.6	Off west coast of Northern Sumatra
11	25.10.2010	14:42:22	3.484°S	100.114°E	20.6	7.7	Kepulaun Mentawai Region, Indonesia
12	3.1.2009	19:43:50	0.408°S	132.886°E	17	7.7	Near North Coast of Papua, Indonesia
13	5.9.2004	10:07:07	33.062°N	136.608°E	14	7.2	Japan
14	29.9.2010	17:11:24	4.920°S	133.783°E	12.3	7.2	Near South Coast of Papua, Indonesia
15	18.6.2010	23:09:31	13.4°N	93.0°E	11	6	Andaman
16	12.6.2010	19:26:46	7.9°N	91.9°E	10	7.8	Off West Coast of Nicobar Islands
17	27.6.2008	11:40:16	11.0°N	91.6°E	10	6.7	Andaman
18	10.8.2008	08:20:34	11.1 N	91.6 E	10	6	Andaman
19	25.3.2007	00:41:57	37.281°N	136.602°E	5	6.7	Japan
20	30.3.2010	16:54:43	13.8°N	92.8°E	4	6.8	Andaman

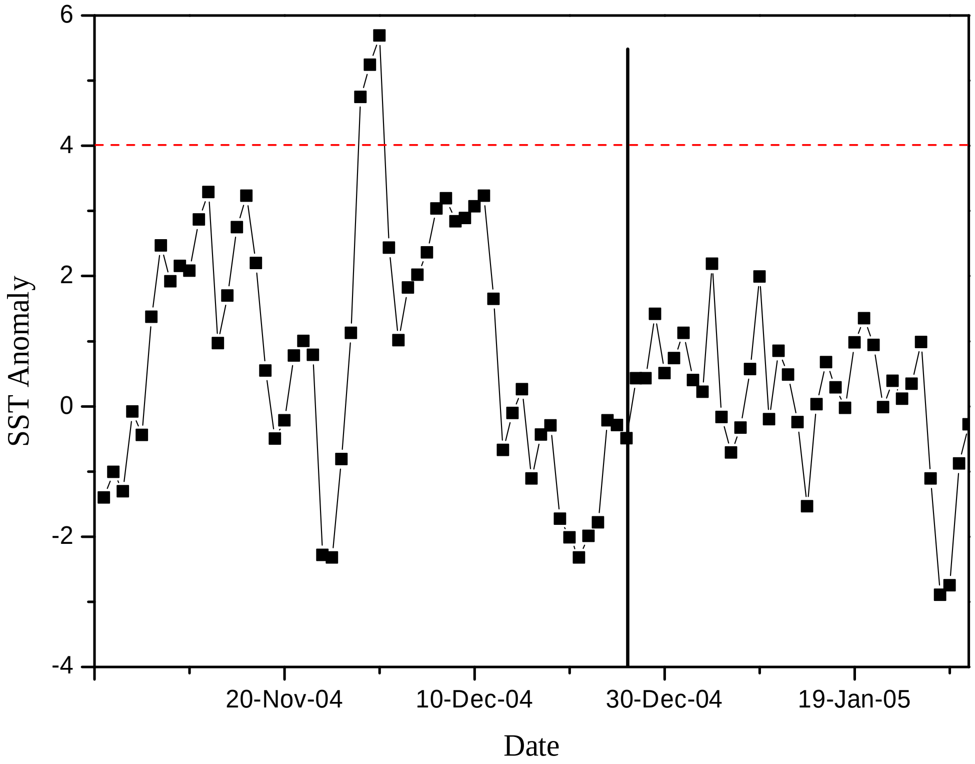

Figure-1
Enhancement in SST 26, 27, 28 days prior to the 26 December 2004 Indonesia EQ of M9.1

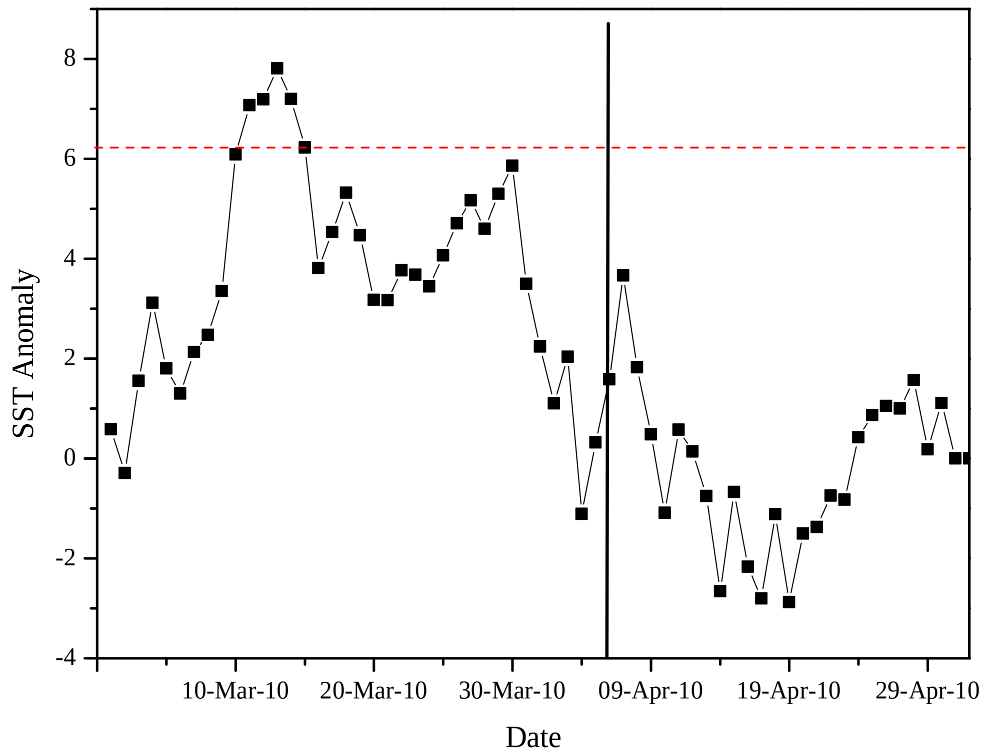

Figure-2
Enhancement in SST 25 days prior to the 6 April 2010 Indonesia EQ of M7.8

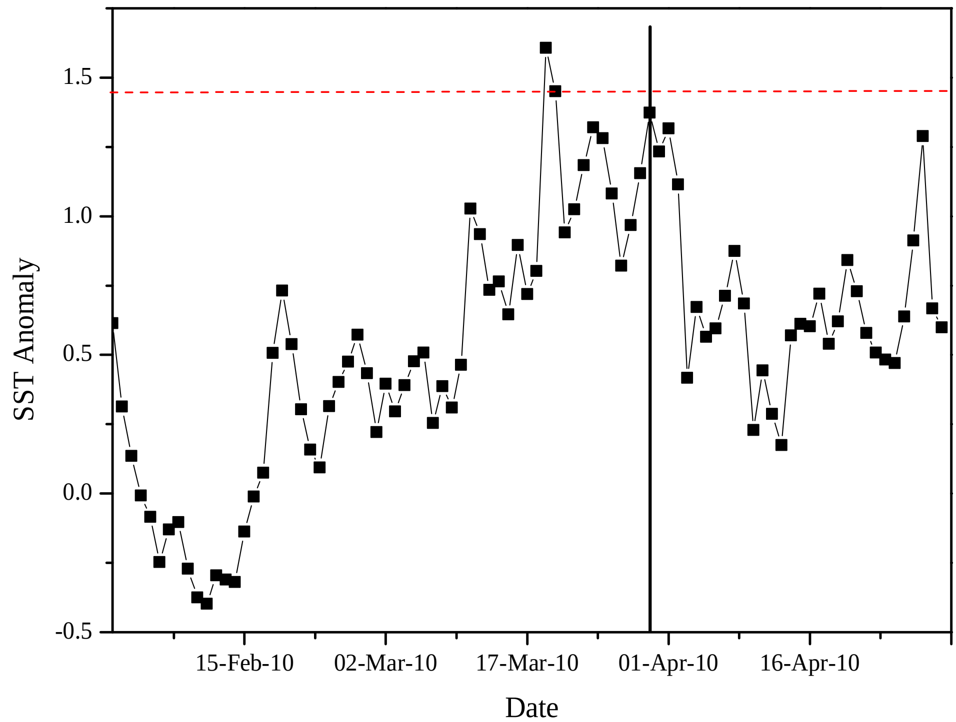

Figure-3
Enhancement in 11 days prior to the 30 March 2010 Andaman EQ of M6.8

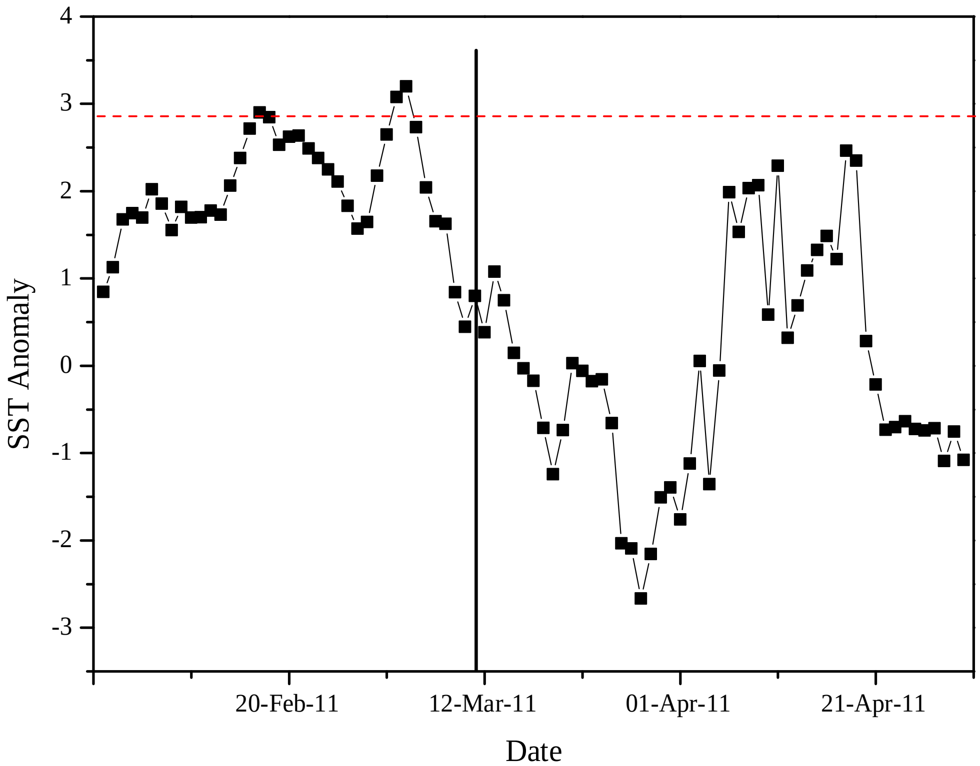

Figure-4
Enhancement in SST 7 days prior to the 11 March 2011 Japan EQ of M9

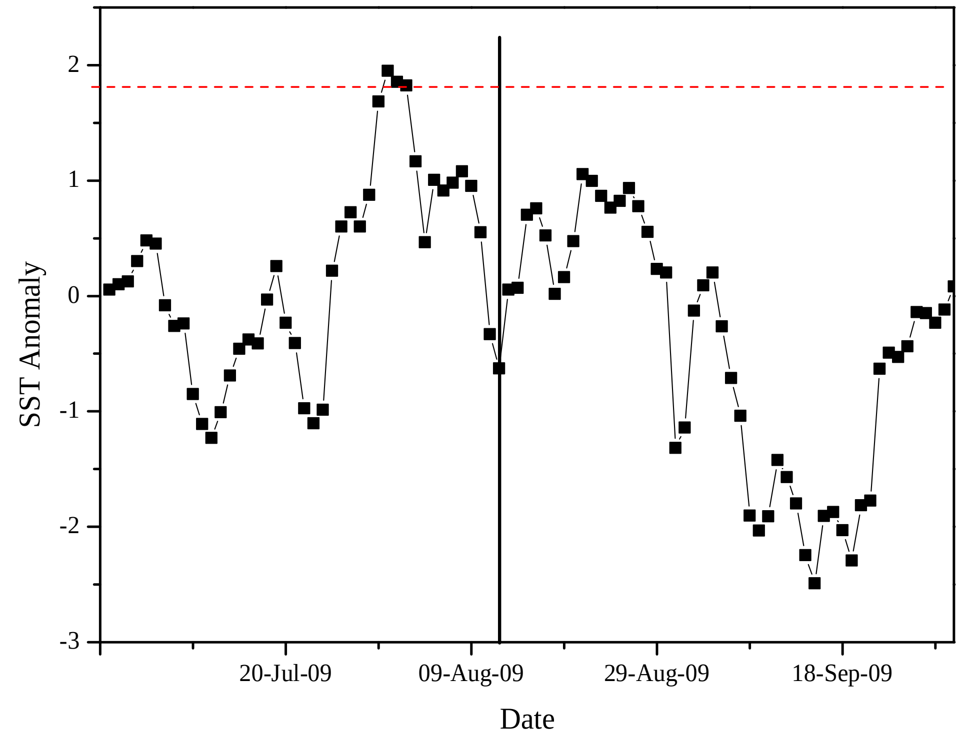

Figure-5
Enhancement in SST 12 days prior to the 12 August 2009 Japan EQ of M6.6

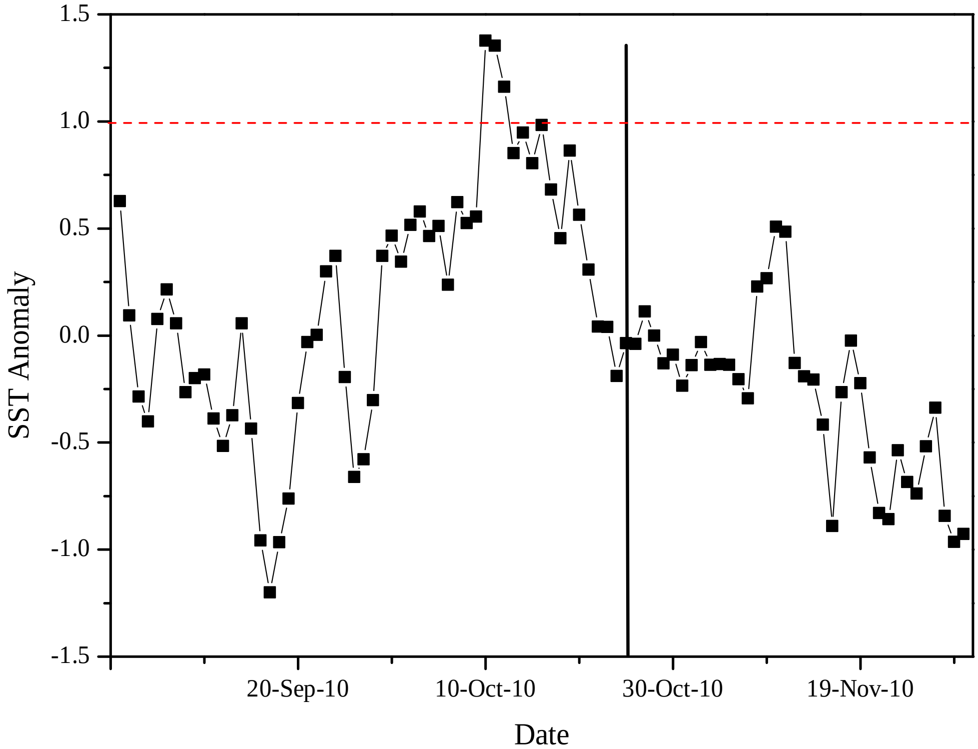

Figure-6
Enhancement in SST 15 days prior to the 25 October 2010 Indonesia EQ of M7.7

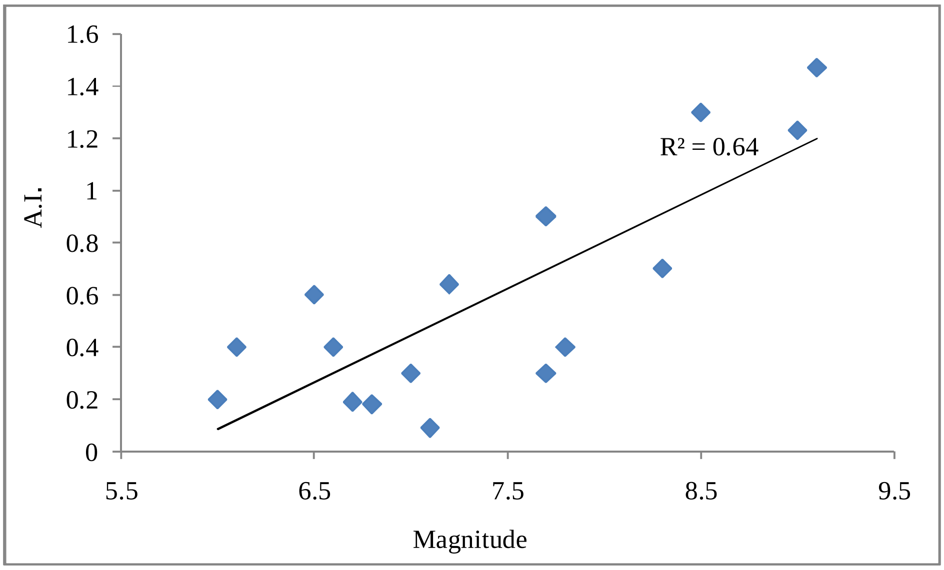

Figure-7
The variation of SST anomaly index with the magnitude of the earthquake. R^2 represents the correlation coefficient

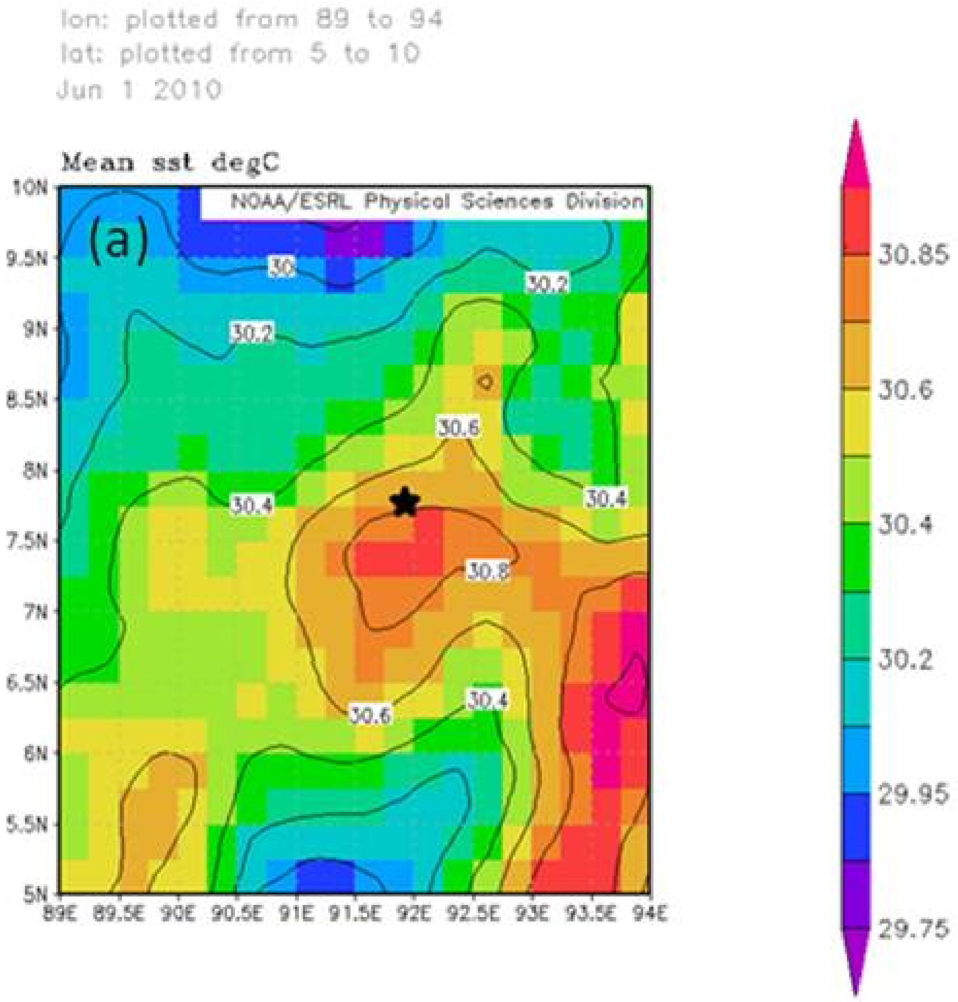

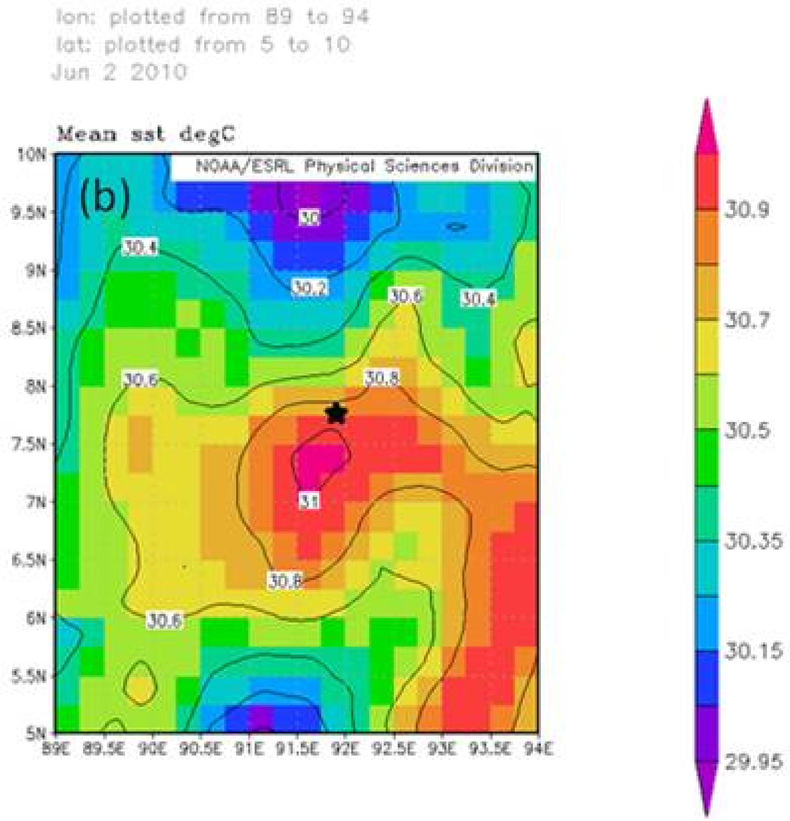
lon: plotted from 89 to 94
lat: plotted from 5 to 10
Jun 2 2010
Mean sst degC
NOAA/ESRL Physical Sciences Division
(b)
30
30.4
30.2
30.6
30.4
30.6
30.8
31
30.8
30.6
30.9
30.7
30.5
30.35
30.15
29.95
10N
9.5N
9N
8.5N
8N
7.5N
7N
6.5N
6N
5.5N
5N
89E 89.5E 90E 90.5E 91E 91.5E 92E 92.5E 93E 93.5E 94E

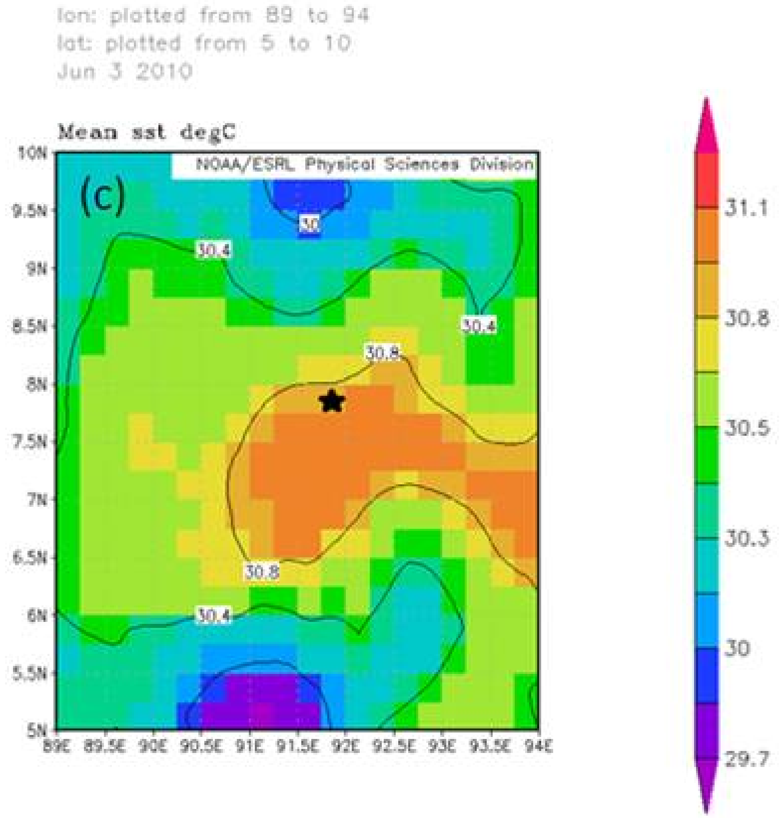
lon: plotted from 89 to 94
lat: plotted from 5 to 10
Jun 3 2010
Mean sst degC
NOAA/ESRL Physical Sciences Division
(c)
30
30.4
30.4
30.8
30.8
30.4
31.1
30.8
30.5
30.3
30
29.7
10N
9.5N
9N
8.5N
8N
7.5N
7N
6.5N
6N
5.5N
5N
89E 89.5E 90E 90.5E 91E 91.5E 92E 92.5E 93E 93.5E 94E

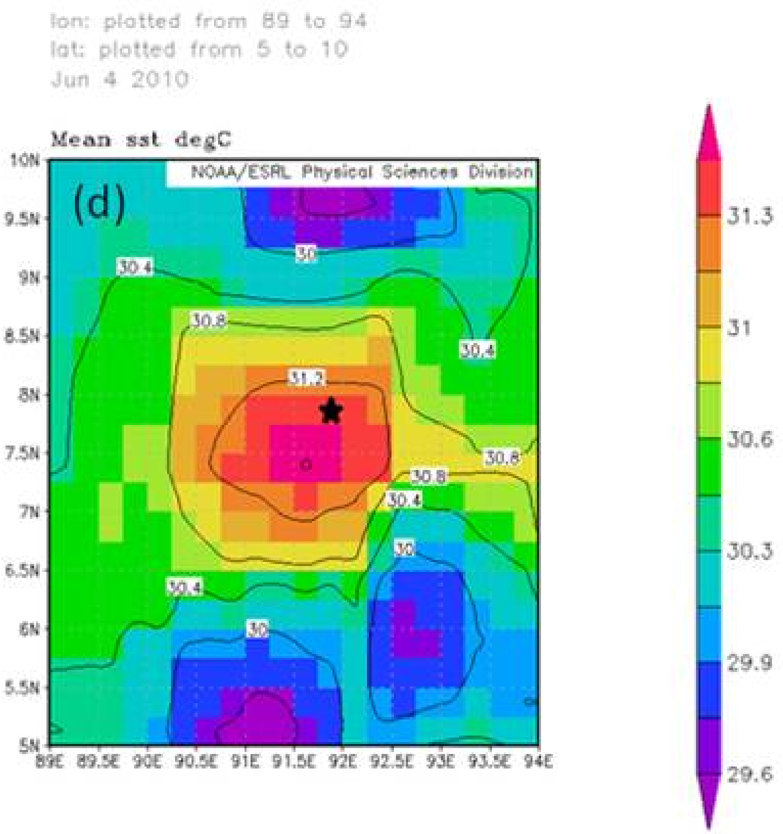
lon: plotted from 89 to 94
lat: plotted from 5 to 10
Jun 4 2010
Mean sst degC
NOAA/ESRL Physical Sciences Division
(d)
31.3
31
30.6
30.3
29.9
29.6

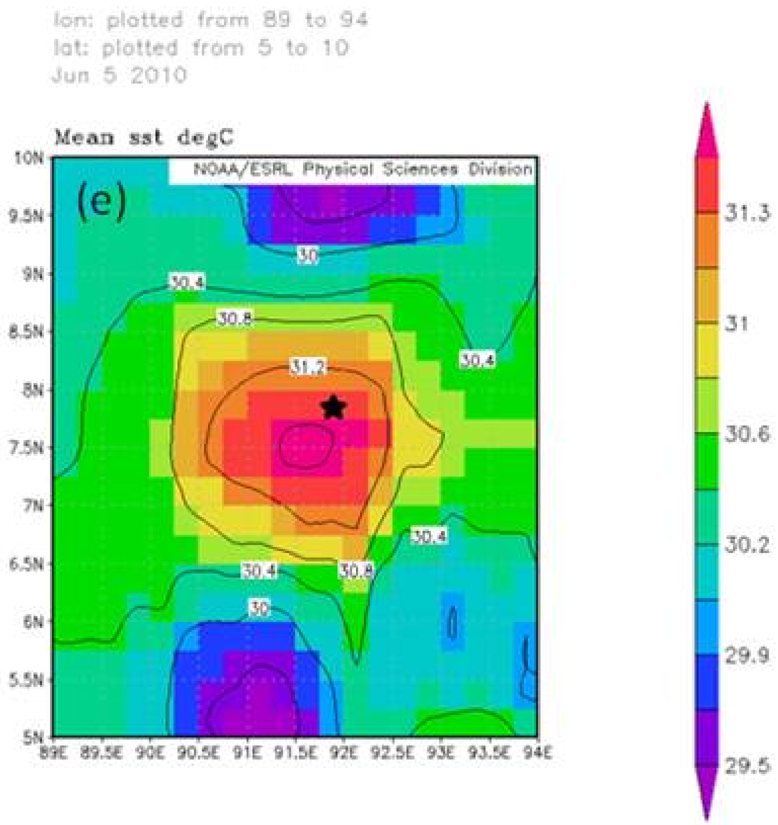
lon: plotted from 89 to 94
lat: plotted from 5 to 10
Jun 5 2010
Mean sst degC
NOAA/ESRL Physical Sciences Division
(e)
31.3
31
30.6
30.2
29.9
29.5

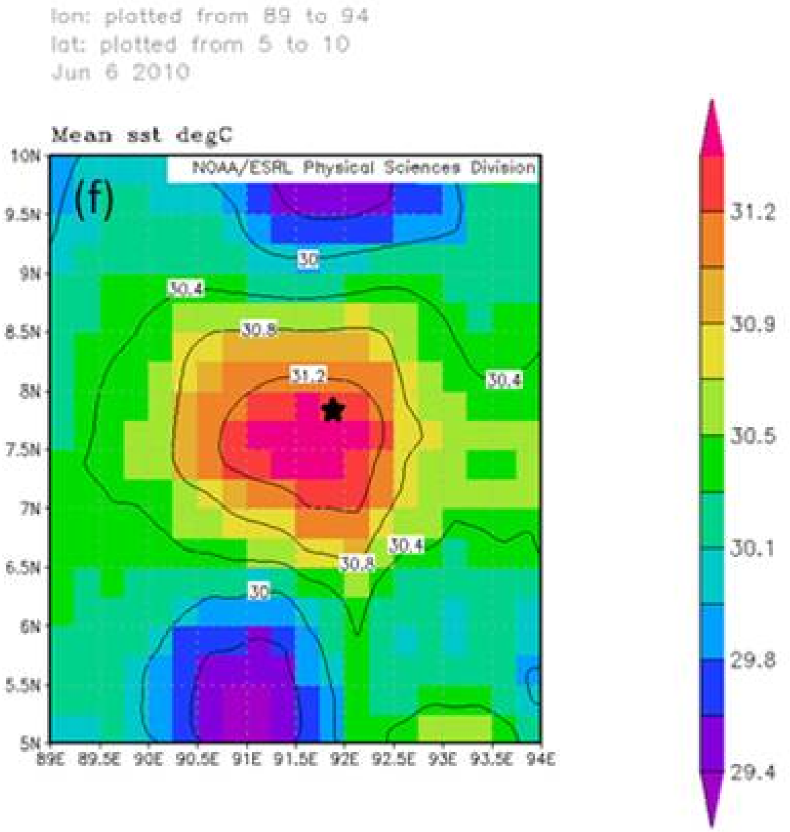
lon: plotted from 89 to 94
lat: plotted from 5 to 10
Jun 6 2010
Mean sst degC
NOAA/ESRL Physical Sciences Division
(f)
30
30.4
30.8
31.2
30.4
30.4
30.8
30
10N
9.5N
9N
8.5N
8N
7.5N
7N
6.5N
6N
5.5N
5N
89E 89.5E 90E 90.5E 91E 91.5E 92E 92.5E 93E 93.5E 94E
31.2
30.9
30.5
30.1
29.8
29.4

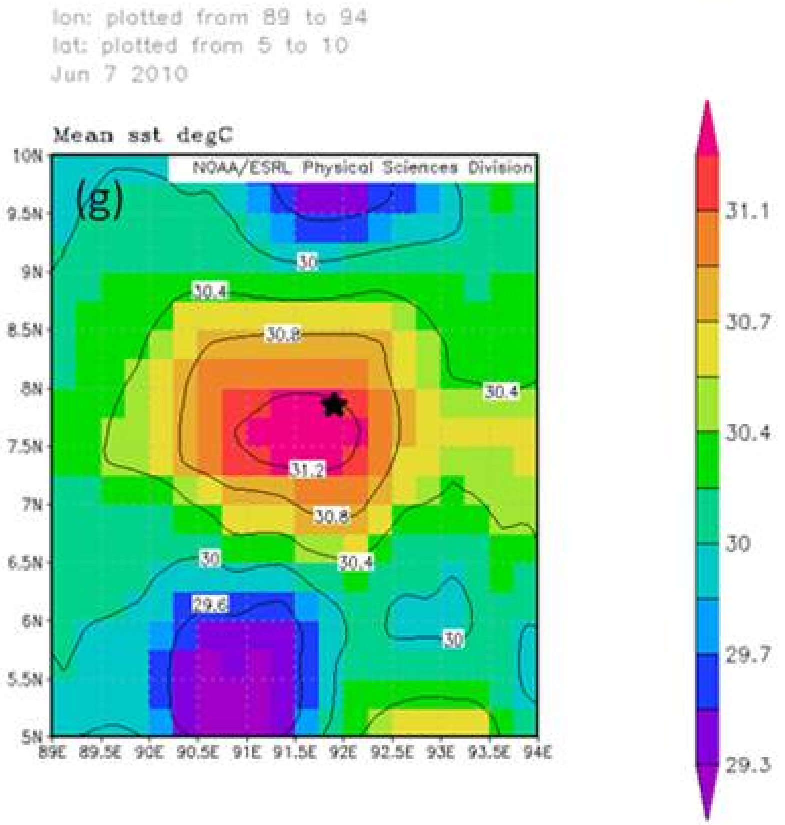
lon: plotted from 89 to 94
lat: plotted from 5 to 10
Jun 7 2010
Mean sst degC
NOAA/ESRL Physical Sciences Division
(g)
30
30.4
30.8
30.4
31.2
30.8
30
30.4
29.6
30
10N
9.5N
9N
8.5N
8N
7.5N
7N
6.5N
6N
5.5N
5N
89E 89.5E 90E 90.5E 91E 91.5E 92E 92.5E 93E 93.5E 94E
31.1
30.7
30.4
30
29.7
29.3

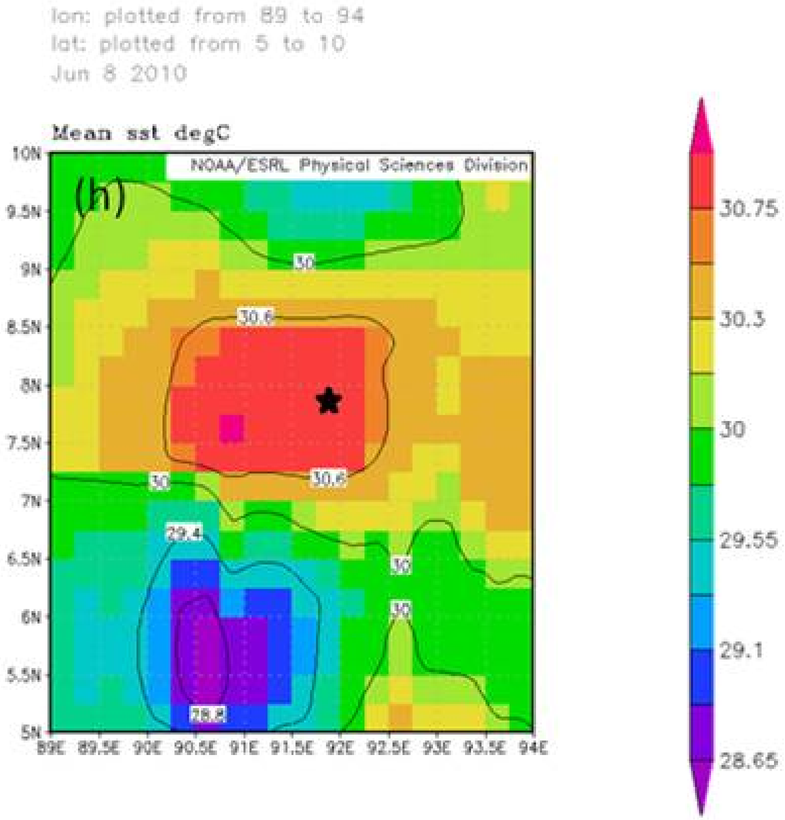
lon: plotted from 89 to 94
lat: plotted from 5 to 10
Jun 8 2010
Mean sst degC
NOAA/ESRL Physical Sciences Division
(h)
30
30.6
30.6
30
29.4
30
30
28.8
10N
9.5N
9N
8.5N
8N
7.5N
7N
6.5N
6N
5.5N
5N
89E 89.5E 90E 90.5E 91E 91.5E 92E 92.5E 93E 93.5E 94E
30.75
30.3
30
29.55
29.1
28.65

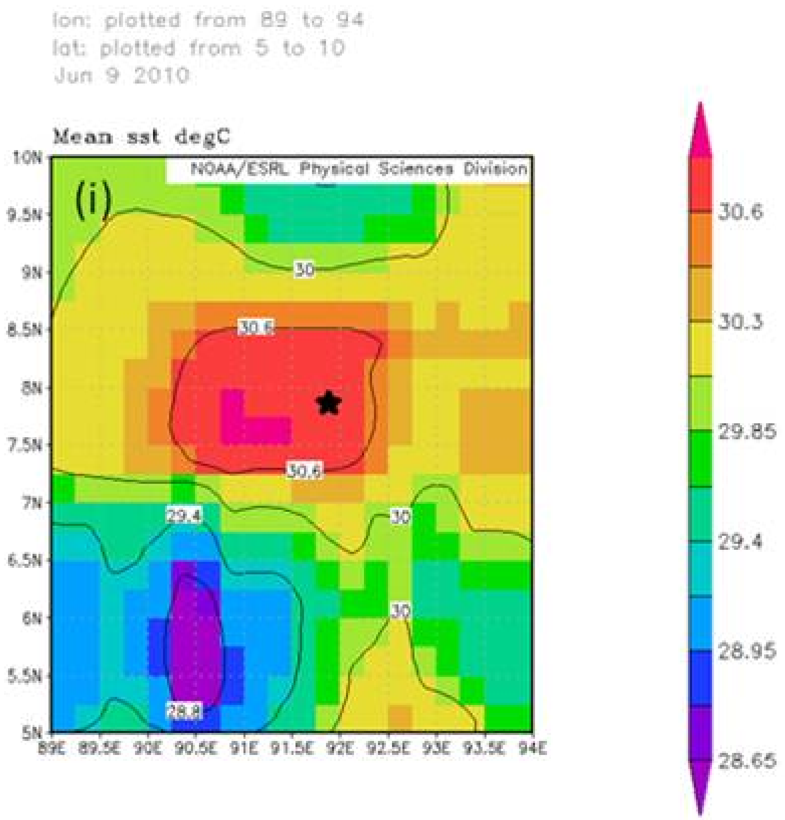
lon: plotted from 89 to 94
lat: plotted from 5 to 10
Jun 9 2010
Mean sst degC
NOAA/ESRL Physical Sciences Division
(i)
30
30.6
30.6
29.4
30
30
28.8
10N
9.5N
9N
8.5N
8N
7.5N
7N
6.5N
6N
5.5N
5N
89E 89.5E 90E 90.5E 91E 91.5E 92E 92.5E 93E 93.5E 94E
30.6
30.3
29.85
29.4
28.95
28.65

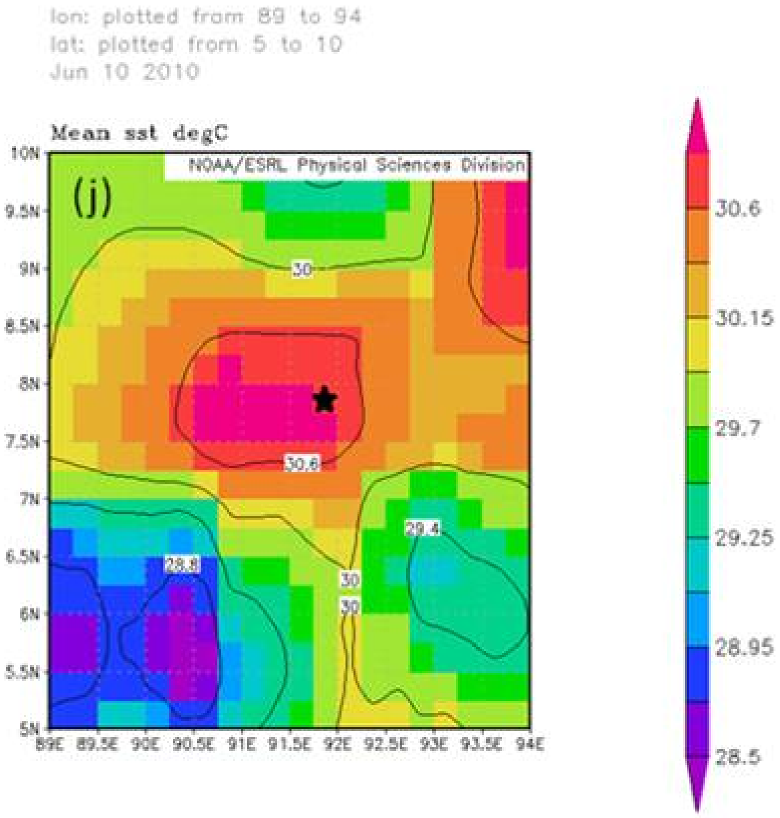
lon: plotted from 89 to 94
lat: plotted from 5 to 10
Jun 10 2010
Mean sst degC
NOAA/ESRL Physical Sciences Division
(j)
30
30.6
29.4
28.8
30
30
10N 9.5N 9N 8.5N 8N 7.5N 7N 6.5N 6N 5.5N 5N
89E 89.5E 90E 90.5E 91E 91.5E 92E 92.5E 93E 93.5E 94E
30.6
30.15
29.7
29.25
28.95
28.5

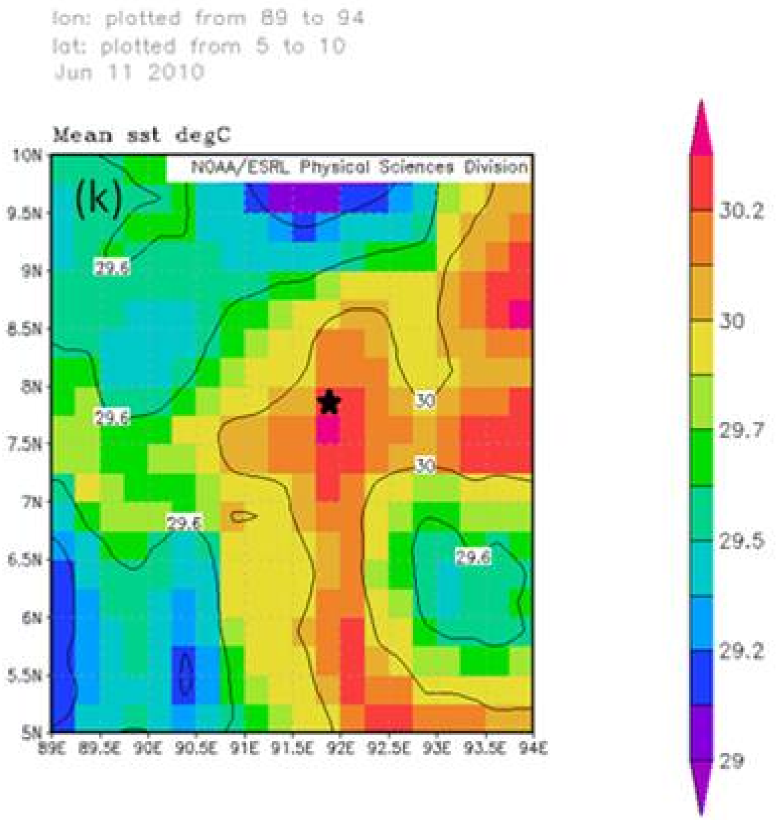
lon: plotted from 89 to 94
lat: plotted from 5 to 10
Jun 11 2010
Mean sst degC
NOAA/ESRL Physical Sciences Division
(k)
29.6
29.6
30
30
29.6
29.6
10N 9.5N 9N 8.5N 8N 7.5N 7N 6.5N 6N 5.5N 5N
89E 89.5E 90E 90.5E 91E 91.5E 92E 92.5E 93E 93.5E 94E
30.2
30
29.7
29.5
29.2
29

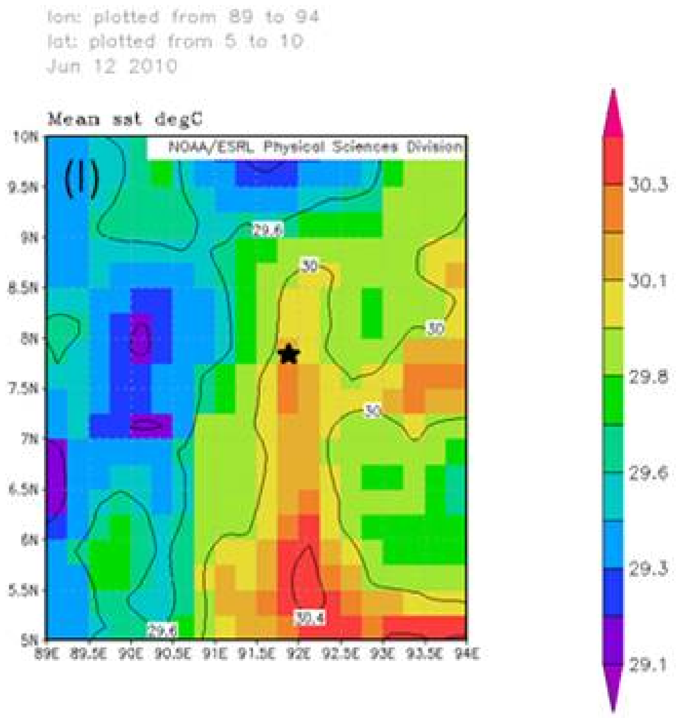

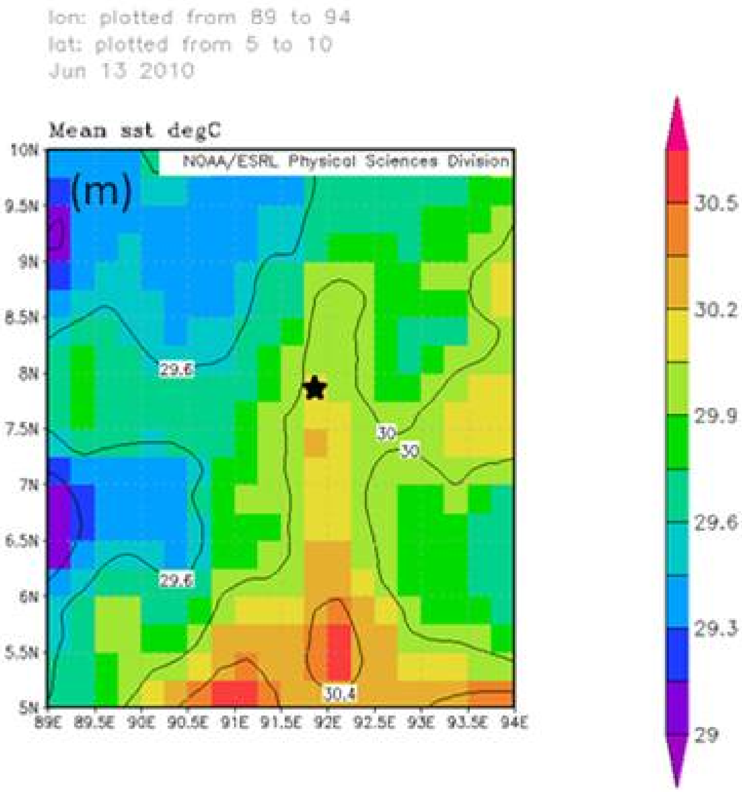

Figure-8(a - m)
The spatial distribution of SST prior to and during 12 June 2010 Nicobar Island EQ of M7.8. The star mark (*) shows the epicenter of earthquake

In figure (9-14) the SLHF anomaly prior to some EQs under consideration are presented. The EQ numbers 4 to 10,12,13,15 to 20 shows anomalous behaviour prior to EQ and EQ numbers 1,2,3,11,14 did not show any change. The SLHF anomaly shows similar trend for all earthquakes. The maximum increase in SLHF has been observed to be 2-16 days prior to the main earthquake event. The variation of maximum value of AI index (A I_{max}) level with the earthquake magnitude is plotted in figure-15 and a significant positive correlation with coefficient of 0.63 is seen between these two parameters. The increase in temperature over the epicentral region prior to the earthquake leads to intense land-ocean-atmosphere interaction giving anomalous SLHF prior to the earthquake. The accumulation of stress prior to the earthquake in the epicentral region is likely to be responsible for the increase in temperature prior to the earthquake. The EQ number 1,2,3 did not show any signature in SLHF prior to EQ as the manifestation of the stress accumulation in terms of surface temperature and SLHF is not prominent in the case of deep focal depth earthquakes[13]. The SLHF is enhanced by the interaction of ocean and atmosphere which is highly dependent on the proximity of the earthquake epicenters to the ocean. The most significant increase in SLHF, observed 1–8 days prior to the earthquake can be associated with the hot fluid ejected from the Earth's crust during the earthquake time. The accumulated heat affects the energy exchange processes; and results in an increase in SLHF prior to the earthquake. After the main earthquake event, the release of accumulated stress shows an immediate decrease in SLHF. The higher moisture content and humidity in the air facilitates the energy transfer to the atmosphere[3]. Here, figure 16(a-k) shows the spatial distribution of the SLHF values in Nicobar region prior to and after the earthquake. The SLHF increases significantly prior to the earthquake. A red color contour is observed near the epicentre prior to EQ. A local anomaly with high amplitude of around 350 W/m^2 is revealed northwest of the epicentre on 7th June 2010. Soon after the earthquake this SLHF contrast is found to disappear on 13th June with value of around 50W/m^2.

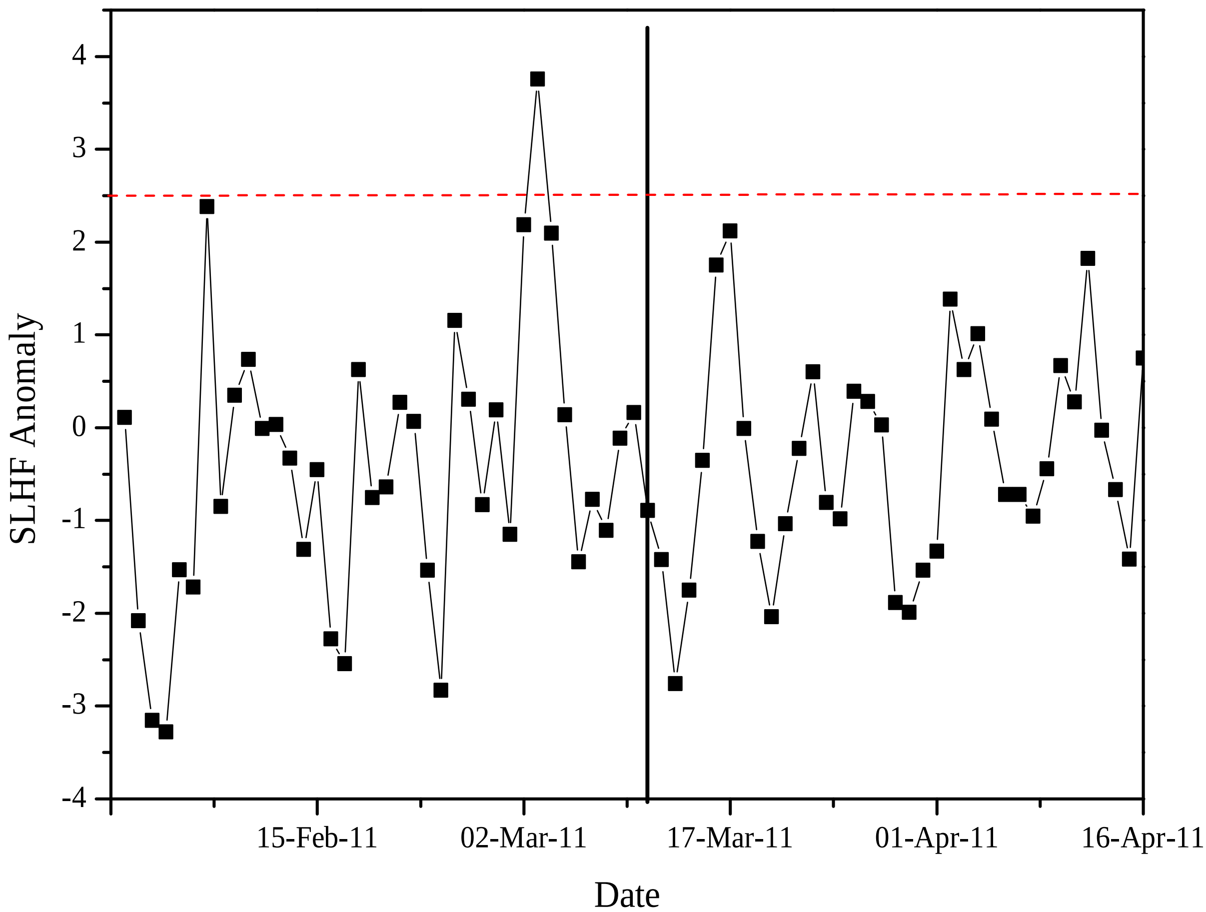

Figure-9
Enhancement in SLHF 8 days prior to the 11 March 2011 Japan EQ of M9

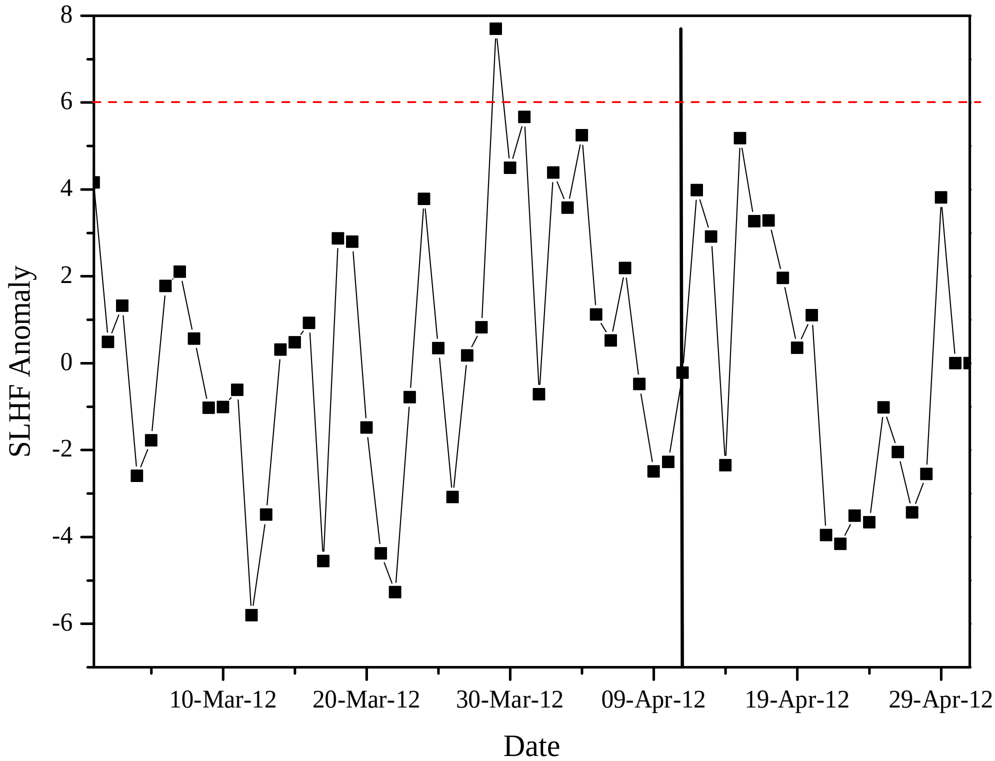

Figure-10
Enhancement in SLHF 13 days prior to the 11 April 2012 Indonesia EQ of M8.5

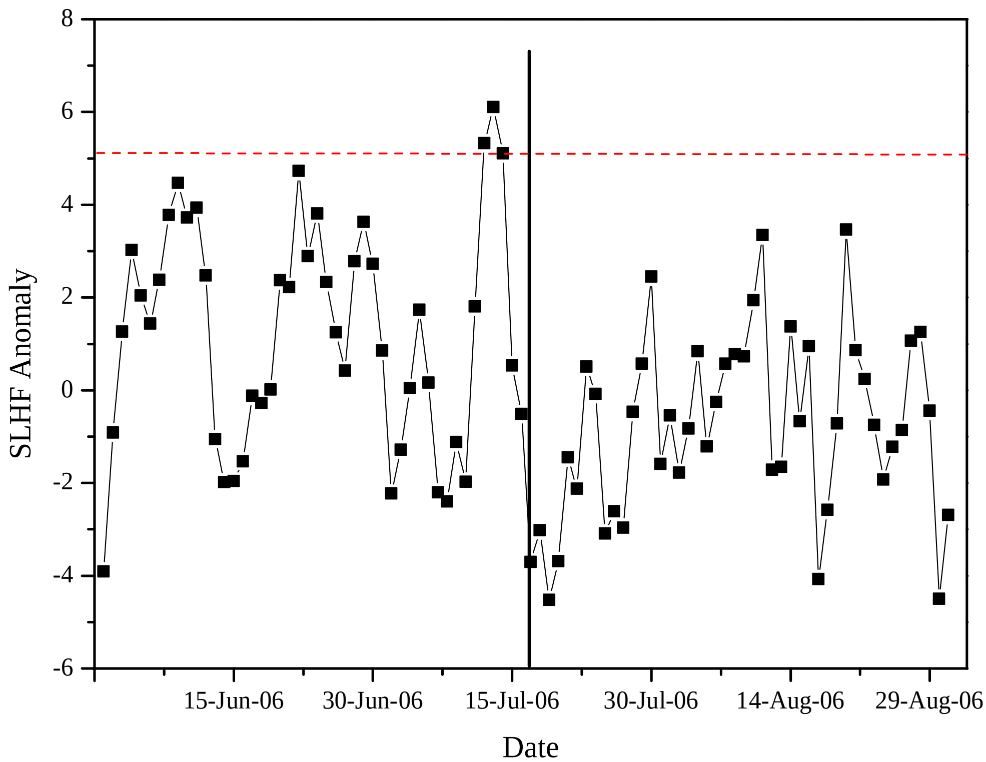

Figure-11
Enhancement in SLHF 4 days prior to the 17 July 2006 Indonesia EQ of M7.7

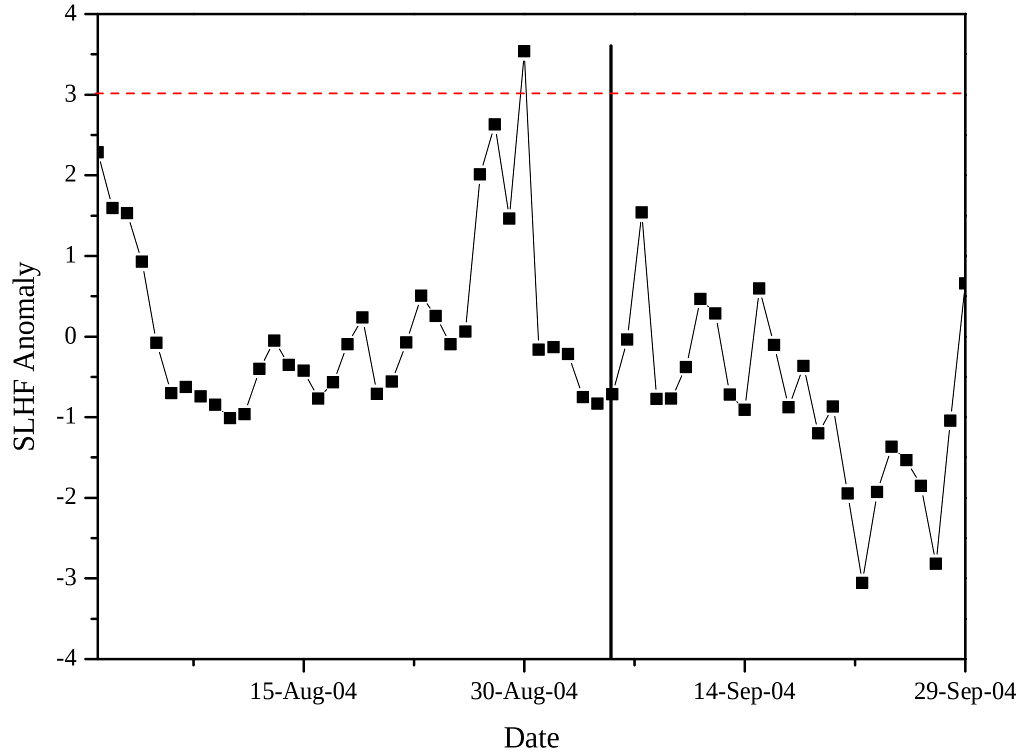

Figure-12
Enhancement in SLHF 7 days prior to the 5.9.2004 Japan EQ of M7.2

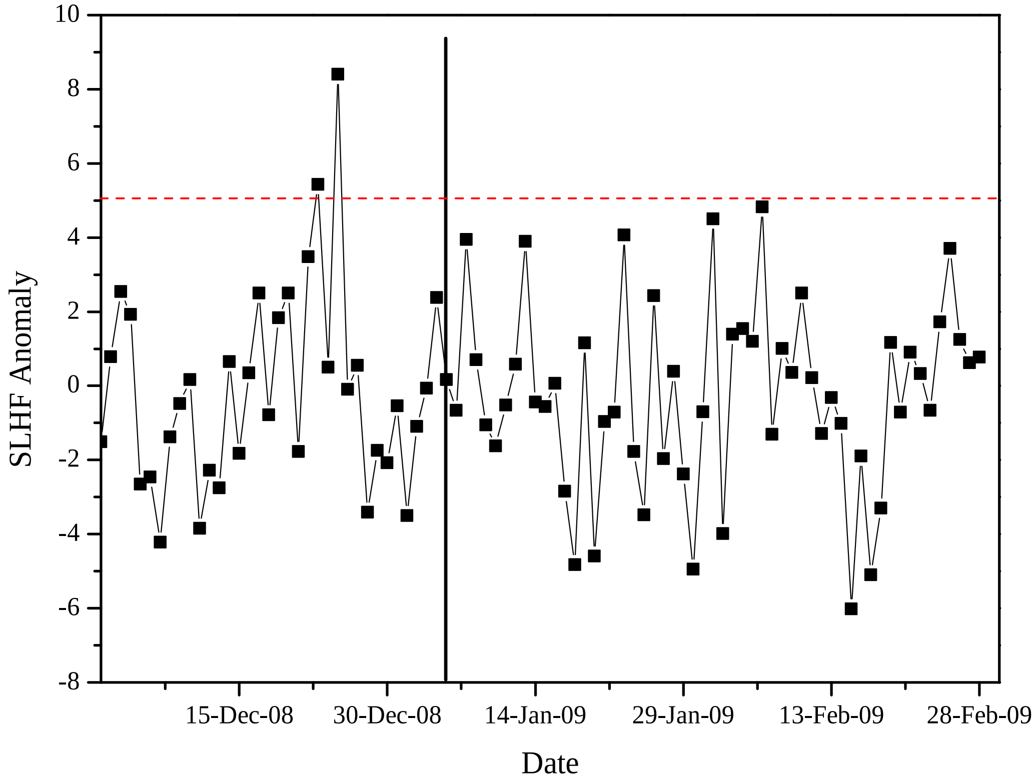

Figure-13
Enhancement in SLHF 11, 13 days prior to the 3.1.2009 Indonesia EQ of M7.7

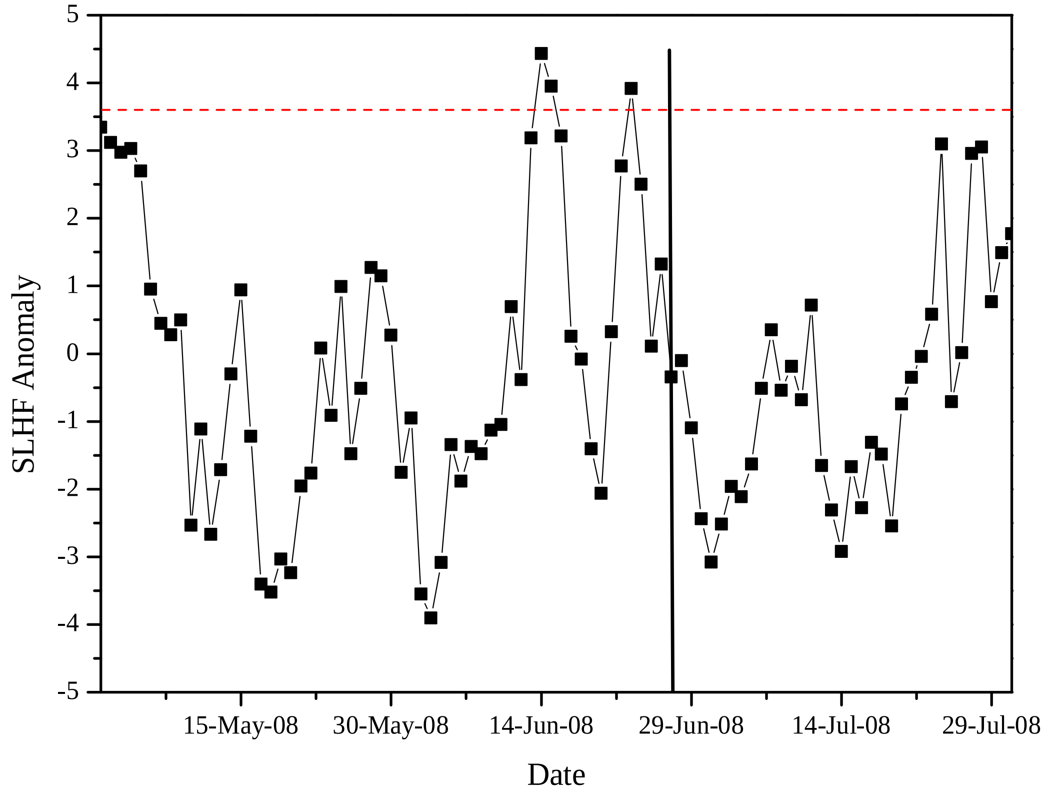

Figure-14
Enhancement in SLHF 4,12,13 days prior to the 27 June 2008 Nicobar Island EQ of M6.7

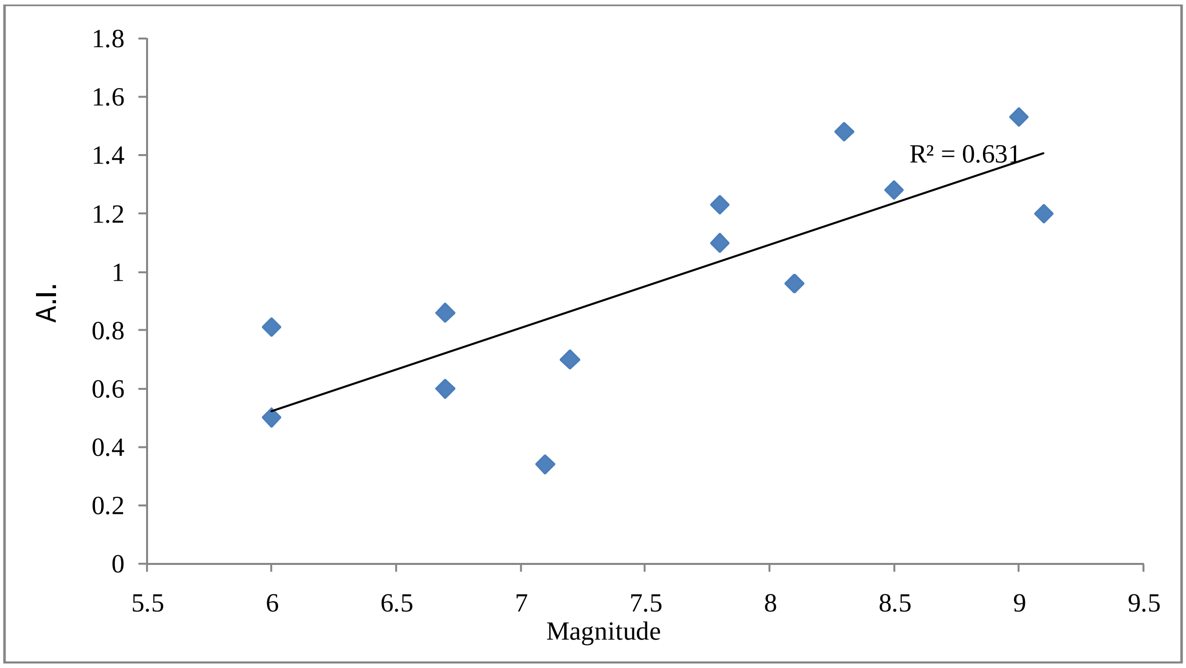

Figure-15
The variation of SLHF anomaly index the magnitude of the earthquake. R^2 represents the correlation coefficient.

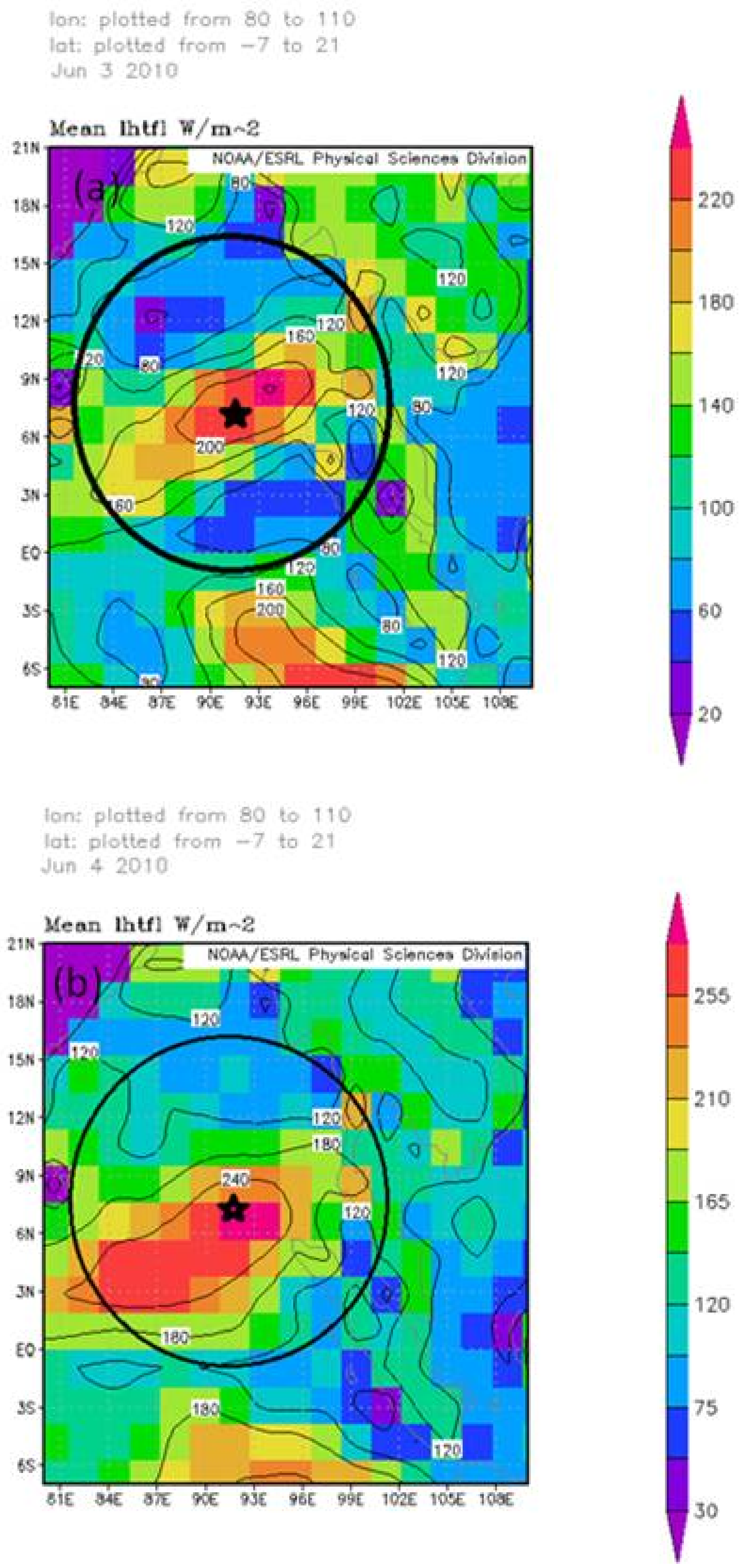
lon: plotted from 80 to 110
lat: plotted from −7 to 21
Jun 3 2010
Mean lhtfl W/m^2
NOAA/ESRL Physical Sciences Division
(a)
21N 18N 15N 12N 9N 6N 3N EQ 3S 6S
81E 84E 87E 90E 93E 96E 99E 102E 105E 108E
220 180 140 100 60 20
lon: plotted from 80 to 110
lat: plotted from −7 to 21
Jun 4 2010
Mean lhtfl W/m^2
NOAA/ESRL Physical Sciences Division
(b)
21N 18N 15N 12N 9N 6N 3N EQ 3S 6S
81E 84E 87E 90E 93E 96E 99E 102E 105E 108E
255 210 165 120 75 30

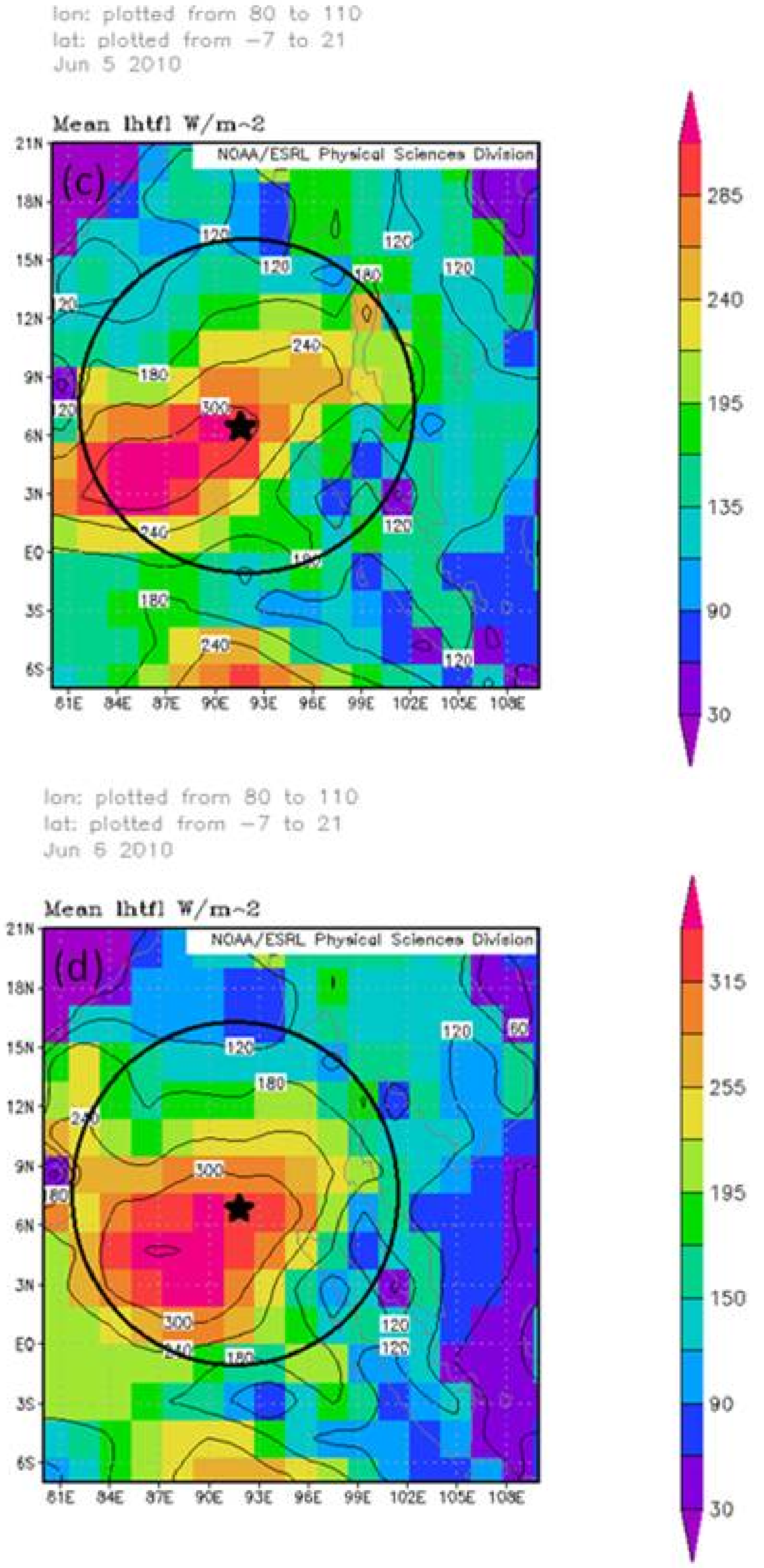
lon: plotted from 80 to 110
lat: plotted from −7 to 21
Jun 5 2010
Mean lhtfl W/m^2
NOAA/ESRL Physical Sciences Division
(c)
21N
18N
15N
12N
9N
6N
3N
EQ
3S
6S
81E 84E 87E 90E 93E 96E 99E 102E 105E 108E
120
180
240
300
285
240
195
135
90
30
lon: plotted from 80 to 110
lat: plotted from −7 to 21
Jun 6 2010
Mean lhtfl W/m^2
NOAA/ESRL Physical Sciences Division
(d)
21N
18N
15N
12N
9N
6N
3N
EQ
3S
6S
81E 84E 87E 90E 93E 96E 99E 102E 105E 108E
60
120
180
240
300
315
255
195
150
90
30

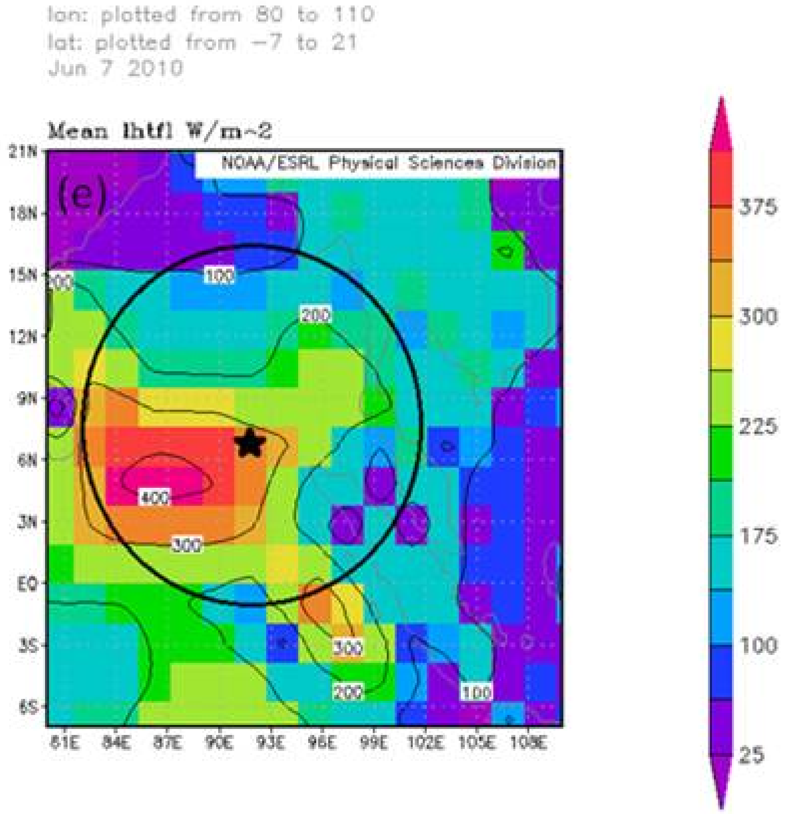
lon: plotted from 80 to 110
lat: plotted from −7 to 21
Jun 7 2010
Mean lhtfl W/m^2
NOAA/ESRL Physical Sciences Division
(e)
21N
18N
15N
12N
9N
6N
3N
EQ
3S
6S
81E 84E 87E 90E 93E 96E 99E 102E 105E 108E
100
200
300
400
375
300
225
175
100
25

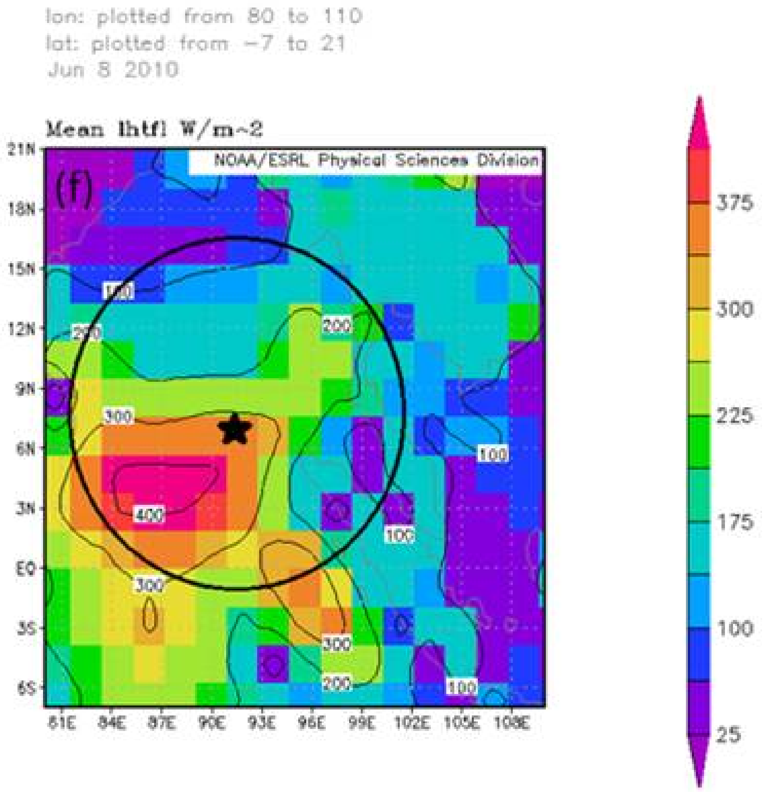
lon: plotted from 80 to 110
lat: plotted from −7 to 21
Jun 8 2010
Mean lhtfl W/m^2
NOAA/ESRL Physical Sciences Division
(f)
21N
18N
15N
12N
9N
6N
3N
EQ
3S
6S
81E 84E 87E 90E 93E 96E 99E 102E 105E 108E
100
200
300
400
375
300
225
175
100
25

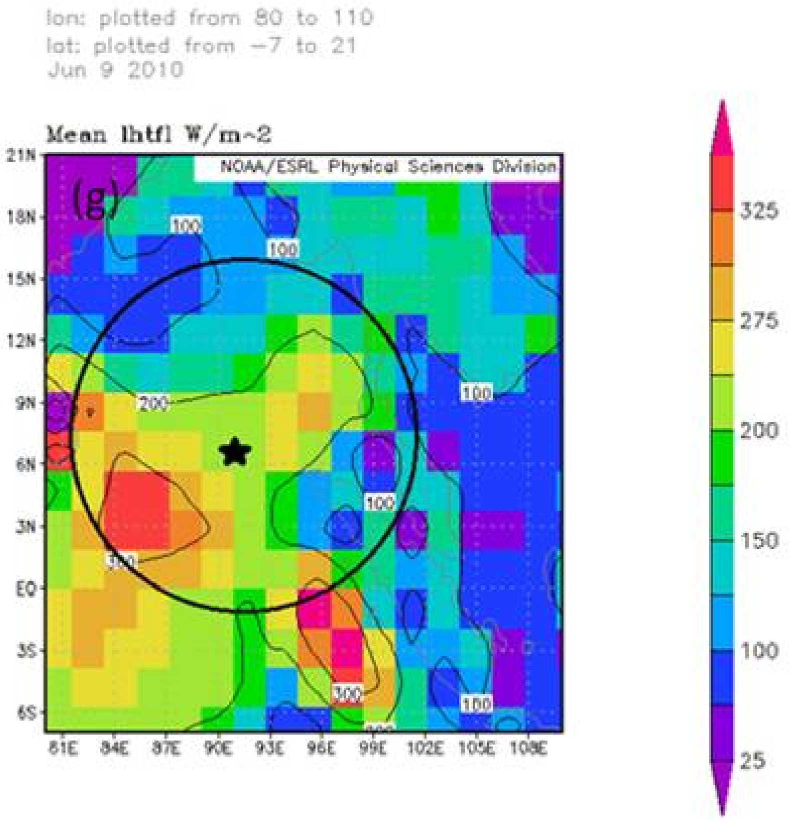
lon: plotted from 80 to 110
lat: plotted from −7 to 21
Jun 9 2010
Mean lhtfl W/m~2
NOAA/ESRL Physical Sciences Division
(g)
325
275
200
150
100
25

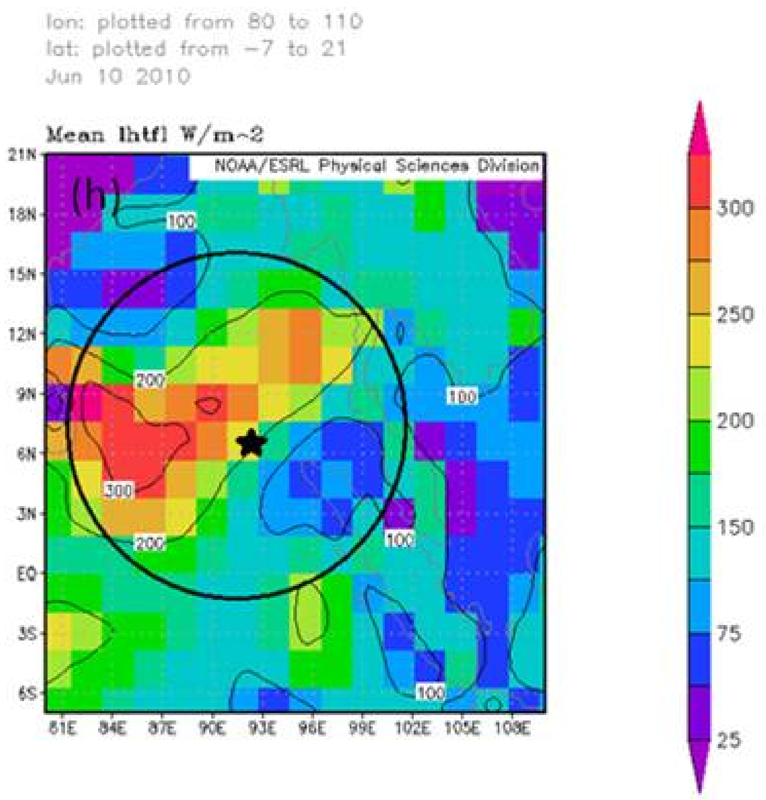
lon: plotted from 80 to 110
lat: plotted from −7 to 21
Jun 10 2010
Mean lhtfl W/m~2
NOAA/ESRL Physical Sciences Division
(h)
300
250
200
150
75
25

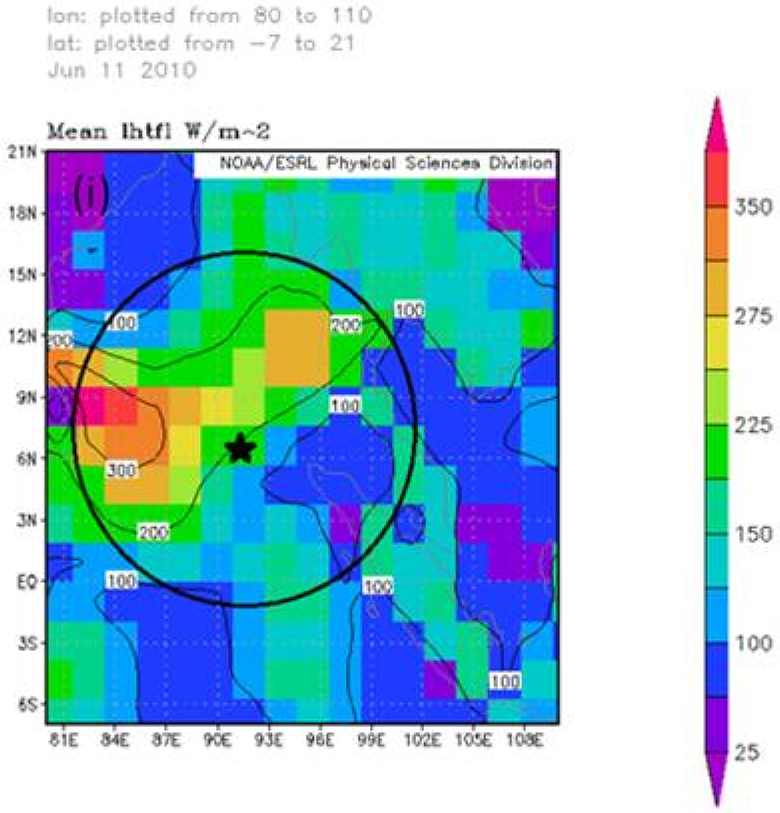
lon: plotted from 80 to 110
lat: plotted from −7 to 21
Jun 11 2010
Mean lhtfl W/m~2
NOAA/ESRL Physical Sciences Division
(i)
21N 18N 15N 12N 9N 6N 3N EQ 3S 6S
81E 84E 87E 90E 93E 96E 99E 102E 105E 108E
100
200
300
350
275
225
150
25

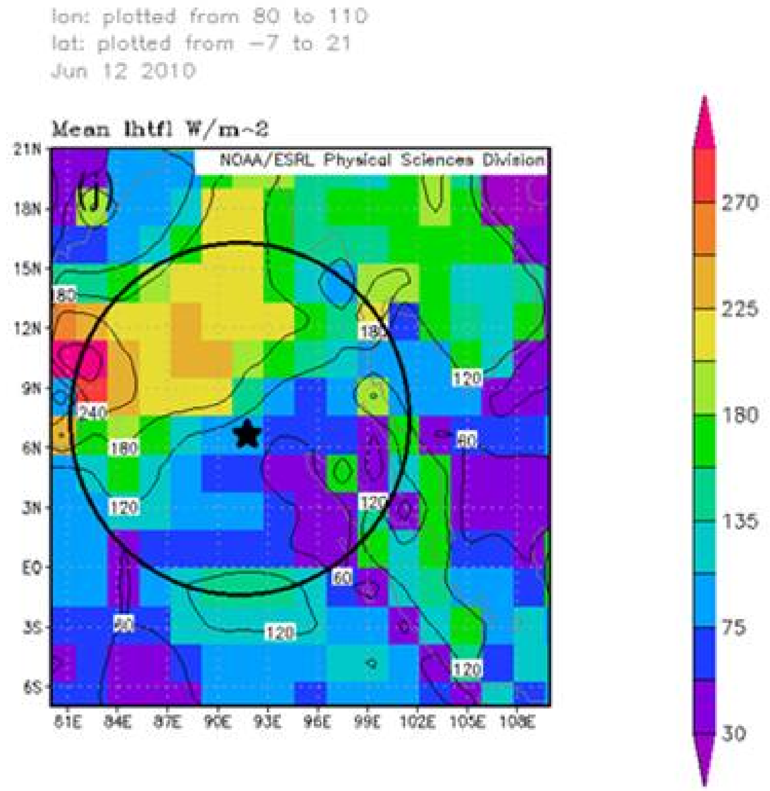
lon: plotted from 80 to 110
lat: plotted from −7 to 21
Jun 12 2010
Mean lhtfl W/m~2
NOAA/ESRL Physical Sciences Division
(j)
21N 18N 15N 12N 9N 6N 3N EQ 3S 6S
81E 84E 87E 90E 93E 96E 99E 102E 105E 108E
180
240
120
60
80
270
225
135
75
30

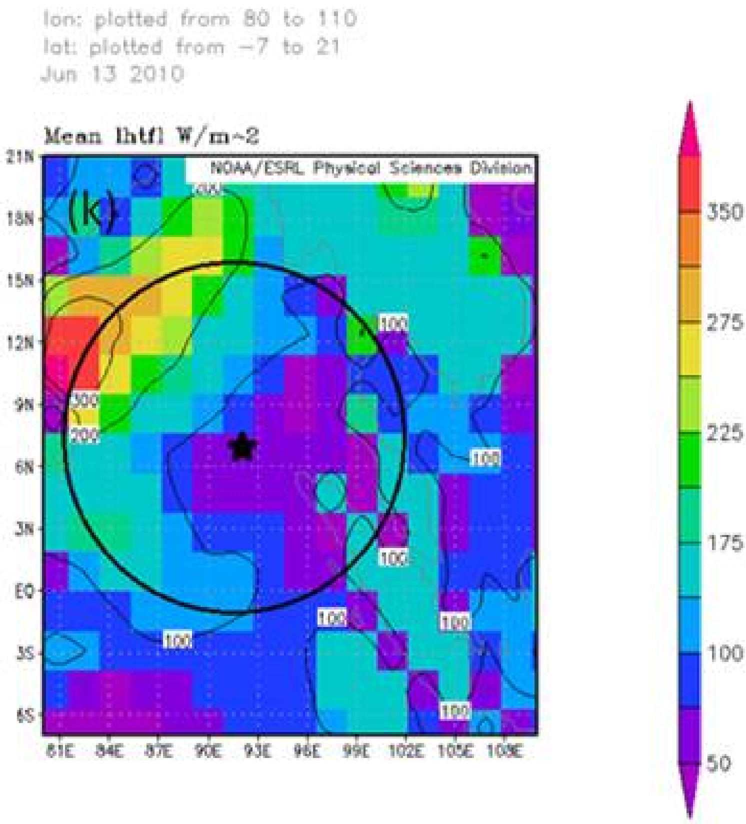

Figure-16(a-k)
The spatial distribution of SLHF prior to and during 12 June 2010 Nicobar earthquake of M7.8. The figure shows SLHF from 3rd June 2010 to 13th June 2010. The star(*) represents the epicenter of earthquake and the black circle represents the earthquake preparatory radius

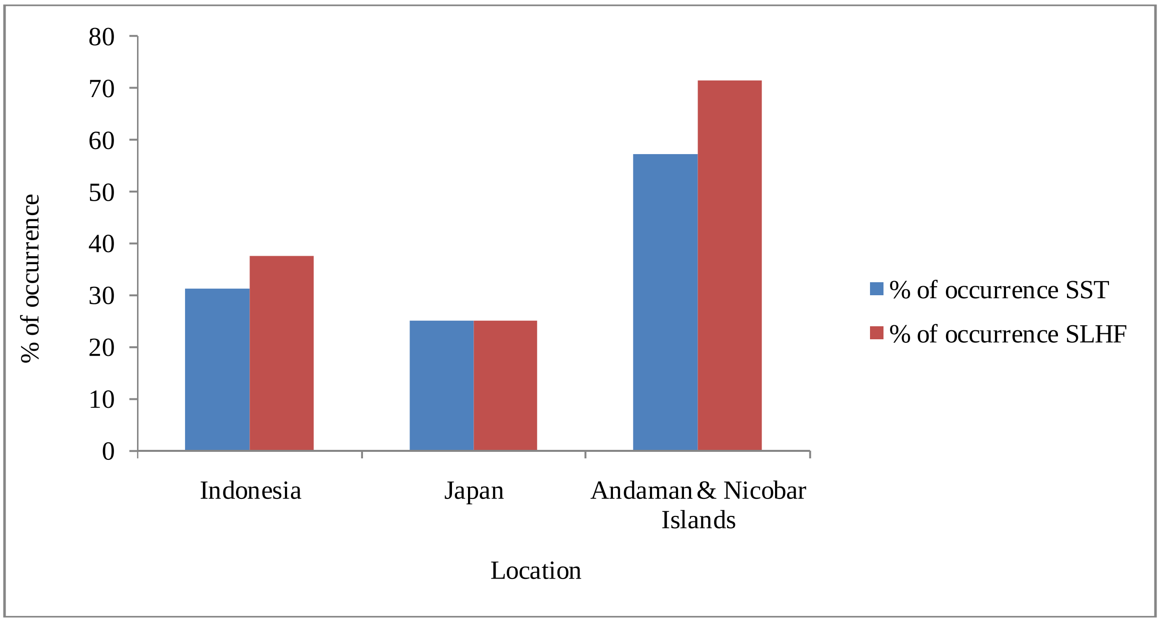

Figure-17
The percentage of occurrence of SST and SLHF in three different locations i.e. Andaman and Nicobar, Indonesia and Japan

Table-2
Results of SST anomaly

Date	Time (UTC)	lat	long	Depth	Mag	Location	SST
12.8.2009	22:48:51	32.816°N	140.382°E	51	6.6	Japan	Y
28.11.2004	18:32:13	42.995°N	145.056°E	39	7	Japan	Y
10.11.2009	02:48:47	08.1°N	92.0°E	36	6.1	Andaman	Y
12.9.2007	11:10:26	4.520°S	101.374°E	34	8.5	Southern Sumatra, Indonesia	Y
17.7.2006	08:19:28	9.222°S	107.320°E	34	7.7	South of Java, Indonesia	Y
6.4.2010	22:15:02	2.360°N	97.132°E	31	7.8	Northern Sumatara, Indonesia	Y
26.12.2004	00:58:53	3.316°N	95.854°E	30	9.1	Northern Sumatara, Indonesia	Y
11.3.2011	05:46:24	38.297°N	142.372°E	30	9	Japan	Y
25.9.2003	19:50:06	41.775°N	143.904°E	27	8.3	Japan	Y
11.4.2012	08:38:37	2.311°N	93.063°E	22.9	8.6	Off west coast of Northern Sumatra	No data
25.10.2010	14:42:22	3.484°S	100.114°E	20.6	7.7	Kepulaun Mentawai Region,Indonesia	Y
3.1.2009	19:43:50	0.408°S	132.886°E	17	7.7	Near North Coast of Papua,Indonesia	N
5.9.2004	10:07:07	33.062°N	136.608°E	14	7.2	Japan	N
29.9.2010	17:11:24	4.920°S	133.783°E	12.3	7.2	Near South Coast of Papua,Indonesia	Y
18.6.2010	23:09:31	13.4°N	93.0°E	11	6	Andaman	Y
12.6.2010	19:26:46	7.9°N	91.9°E	10	7.8	Off West Coast of Nicobar Islands	Y
27.6.2008	11:40:16	11.0°N	91.6°E	10	6.7	Andaman	Y
10.8.2008	08:20:34	11.1 N	91.6 E	10	6	Andaman	Y
25.3.2007	00:41:57	37.281°N	136.602°E	5	6.7	Japan	N
30.3.2010	16:54:43	13.8°N	92.8°E	4	6.8	Andaman	Y

Table-3
Results of SLHF anomaly

Date	Time (UTC)	lat	long	Depth	Mag	Location	SLHF
12.8.2009	22:48:51	32.816°N	140.382°E	51	6.6	Japan	N
28.11.2004	18:32:13	42.995°N	145.056°E	39	7	Japan	N
10.11.2009	02:48:47	08.1°N	92.0°E	36	6.1	Andaman	N
12.9.2007	11:10:26	4.520°S	101.374°E	34	8.5	Southern Sumatra, Indonesia	Y
17.7.2006	08:19:28	9.222°S	107.320°E	34	7.7	South of Java, Indonesia	Y
6.4.2010	22:15:02	2.360°N	97.132°E	31	7.8	Northern Sumatara, Indonesia	Y
26.12.2004	00:58:53	3.316°N	95.854°E	30	9.1	Northern Sumatara, Indonesia	Y
11.3.2011	05:46:24	38.297°N	142.372°E	30	9	Japan	Y
25.9.2003	19:50:06	41.775°N	143.904°E	27	8.3	Japan	Y
11.4.2012	08:38:37	2.311°N	93.063°E	22.9	8.6	Off west coast of Northern Sumatra	Y
25.10.2010	14:42:22	3.484°S	100.114°E	20.6	7.7	Kepulaun Mentawai Region,Indonesia	N
3.1.2009	19:43:50	0.408°S	132.886°E	17	7.7	Near North Coast of Papua,Indonesia	Y
5.9.2004	10:07:07	33.062°N	136.608°E	14	7.2	Japan	Y
29.9.2010	17:11:24	4.920°S	133.783°E	12.3	7.2	Near South Coast of Papua,Indonesia	N
18.6.2010	23:09:31	13.4°N	93.0°E	11	6	Andaman	Y
12.6.2010	19:26:46	7.9°N	91.9°E	10	7.8	Off West Coast of Nicobar Islands	Y
27.6.2008	11:40:16	11.0°N	91.6°E	10	6.7	Andaman	Y
10.8.2008	08:20:34	11.1 N	91.6 E	10	6	Andaman	Y
25.3.2007	00:41:57	37.281°N	136.602°E	5	6.7	Japan	Y
30.3.2010	16:54:43	13.8°N	92.8°E	4	6.8	Andaman	Y

The results of SST and SLHF anomaly are shown in table-2 and table-3. In figure-17 the percentage of occurrence of SST and SLHF in Andaman and Nicobar Island, Indonesia and Japan are presented. It is seen that the percentage of occurrence of both SST and SLHF is maximum in Andaman and Nicobar region.

Conclusion

The analysis of SST and SLHF data of the earthquakes under consideration shows anomalous behaviour prior to earthquake. Such anomalous behaviour is found to be associated with coastal earthquakes. Thus, from the results it is noted that SST increases 2-3 weeks prior to EQ and on the other hand SLHF increases 2-16 days prior to the EQ. The SST anomaly is found to be most significant in case of Indonesia earthquakes and least in case of Japan. This could be due the influence of the two ocean currents Kuroshio currents and Oyashio Current near Japan. Both SST and SLHF show good co-relation with earthquake. The percentage of occurrence of SST and SLHF anomaly is maximum in case of Andaman and Nicobar earthquakes followed by Indonesian Earthquakes and least in case of Japan Earthquakes. This may be due to the fact that Indonesia and Japan are situated in the fault zone and Andaman is situated in the off-fault region. It may also be related to the latitude of the place. This is yet to be explored. So, we can conclude that the parameters SST and SLHF can be used for study of earthquake precursor. The systematic pattern of SST and SLHF show a potential precursor to provide information about disastrous earthquakes. The high resolution remote sensing data with better spatial and temporal resolutions may provide more reliable information about SST, which can be easily used, for early warning of coastal earthquakes.

Acknowledgement

Authors acknowledge NCEP site (http://iridl.columbia.edu) and NCEP (http://iridl.ldeo.columbia.edu/ SOURCES/. NOAA /.NCDC /.OISST) for downloading surface latent heat flux data and sea surface temperature data.

References

1. Alvan H.V., Azad F.H. and Mansor S., Latent heat flux and air temperature anomalies along an active fault zone associated with recent Iran earthquakes, *Adv. in Space Research*, **52**, 1678-1687 **(2013)**
2. Dey S., Sarkar S., and Singh R.P., Anomalous changes in column water vapor after Gujarat earthquake, *Adv. Space R.*, **33**, 274-278 (**2004)**
3. Gorny V.I., Salman A.G. and Tronin A.A., The Earth's outgoing IR radiation as an indicator of seismic activity, *Proc. Acad.Sci. USSR,* **301**, 67-69 **(1988)**
4. Ouzounov, D. and Freund F., Mid-infrared emission prior to strong earthquakes analyzed by remote sensing data. *Adv. Space Res.*, **33**, 268-273 **(2004)**
5. Qiang Z., Thermal infrared anomoly precursor of impending earthquakes, *Pure and Applied Geophysics*, **149**, 159–170 (**1997**)
6. Qin K., Wu L. X., De Santis A., and Wang H., Surface latent heat flux anomalies before the Ms7.1 New Zealand earthquake 2010, *Chinese Sci. Bull*., **56**, 3273–3280 (**2011)**
7. Qin K., Wu L. X., Ouyang X. Y., Shen X. H. and Zheng S., Surface latent heat flux anomalies quasi-synchronous with ionospheric disturbances before the 2007 Pu'er earthquake in China, *Adv. Space Res.*, **53**, 266–271 (**2014**)
8. Singh R.P., Bhoi S. and Sahoo A.K., Significant changes in the ocean parameters after the Gujarat earthquake, *Current Science*, **80(a)**, 1376- 1377 **(2001)**
9. Singh R.P., Bhoi S., and Sahoo A.K., Raj U. and Ravindran S., Surface manifestations after the Gujarat earthquake, *Current Science,* **81(b)**, 164-166 **(2001)**
10. Cervone G., Kafatos M., Napoletani D. and Singh R.P., Wavelet maxima curves of surface latent heat flux associated with two recent Greek earthquakes, *Nat. Hazards Earth Syst. Sci.*, **4**, 359–374 (**2004)**
11. Goswami H., Devi M., Choudhury B and Barbara A.K., Meteorological perturbation Observed in the Earthquake Preparatory Zone before Great Earthquakes, *Journal of the Assam Science Society,* (ISSN: 0587-1921) **(2012)**
12. Saraf A.K. and Choudhury S, Thermal Remote Sensing Technique in the Study of Pre-Earthquake Thermal Anomalies, *J. Ind. Geophys. Union***., 9(3)**, 197-207 **(2005)**
13. Dey S. and Singh R.P., Surface latent heat flux as an earthquake precursor, *Nat. Hazards earth Syst. Sci.*, **3**, 1-7 (**2003)**
14. http://iridl.ldeo.columbia.edu/, **(2015)**
15. http://earthquake.usgs.gov/ activity/world.Html, **(2015)**